



Shared metamorphic histories of various Palaeoproterozoic granulites from Datong–Huai’an area, North China Craton (NCC): constraints from zircon U–Pb ages and petrology

Jialin Wu^{a,b}, Huafeng Zhang^c, Mingguo Zhai^{d,e}, Hong Zhang^b, Haozheng Wang^f, Rongxi Li^a, Bo Hu^a and Haidong Zhang^a

^aSchool of Earth Science and Resources, Chang’an University, Xi’an, China; ^bState Key Laboratory of Continental Dynamics, Department of Geology, Northwest University, Xi’an, China; ^cSchool of Earth Sciences and Resources, China University of Geosciences, Beijing, China; ^dKey Laboratory of Computational Geodynamics, University of Chinese Academy of Sciences, Beijing, China; ^eInstitute of Geology and Geophysics, Chinese Academy of Sciences, Beijing, China; ^fSchool of Geoscience and Technology, Southwest Petroleum University, Chengdu, China

ABSTRACT

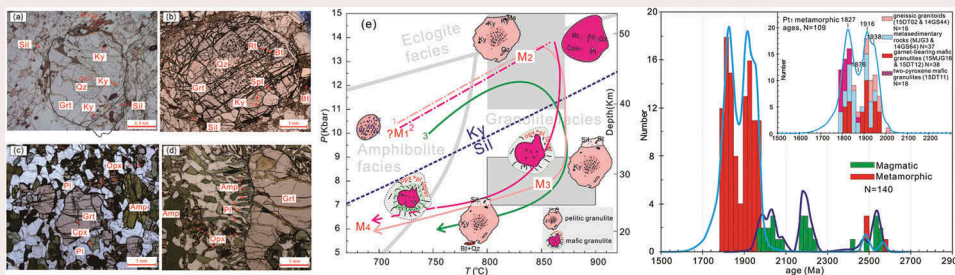
Different tectonic interpretations have been proposed for the various spatially associated Palaeoproterozoic granulite-facies lithologies (metasedimentary rocks, metabasites, and felsic granulites) from north-central part of the North China Craton, which hinges primarily on controversies about metamorphic histories of these granulites, especially on the timing of peak metamorphism. Published data exhibit two controversial peak metamorphic ages of 1950–1900 Ma and 1850–1800 Ma. We report here LA-ICPMS U–Pb zircon ages of seven representative granulite-facies samples of different lithologies to constrain the timing of metamorphism, and then discuss their geological significance. Most zircon grains from these rocks display weak core-and-rim structures and yield two comparable group metamorphic ages of 1970–1900 Ma and 1880–1790 Ma, although their formation ages vary from Neoproterozoic to Palaeoproterozoic. The older population metamorphic ages are interpreted to approximate timing of high-pressure granulite-facies metamorphism, and the younger population ages as the approximate timing of intermediate- to low-pressure granulite-facies metamorphism. Combined with recent petrological studies, we propose these granulites have shared metamorphic histories at least since ~1970–1900 Ma, and they are probably formed in one single metamorphic cycle in response to crustal-scale subduction–collision–exhumation processes involved in Palaeoproterozoic mobile belt.

ARTICLE HISTORY

Received 9 October 2017
Accepted 3 March 2018

KEYWORDS

Zircon U–Pb ages;
Palaeoproterozoic granulites;
shared metamorphic
histories; Datong–Huai’an
area; North China Craton



1. Introduction

The North China Craton (NCC) is one of the oldest cratons in the world, which registers a long, evolving, and complex history of the earth. It witnesses the formation of continental nucleus, growth of continental crust, amalgamation of microblocks and Neoproterozoic Great Oxidation Event and mobile belts, Meso-Neoproterozoic magmatic events

and multistage rifting, Palaeozoic orogenesis at northern and southern margins of the NCC, and Mesozoic lithospheric thinning of the eastern NCC (Zhai and Santosh 2011, 2013; Zhai *et al.* 2015; and reference therein).

The Palaeoproterozoic granulite-facies lithologies (metasedimentary rocks, metabasites, and felsic granulites) in north-central part of the NCC have attracted broad attentions over the past two decades, which offer

important clues to understanding final cratonization and reconstruction of early Precambrian plate tectonics in the NCC (e.g. Zhao *et al.* 2006, 2010, 2012; Zhai 2009, 2012; Santosh *et al.* 2012; Guo *et al.* 2015; Wu *et al.* 2016, 2017; Zhang *et al.* 2016a; Zhou *et al.* 2017; and reference therein). However, due to high-temperature re-equilibrium and multistages metamorphic overprint, the varying granulites documented variable metamorphic assemblages, mineral compositions, and isotopic records, which led to controversies on P - T evolution, timing, and hence different interpretations on petrogenetic relations and tectonic implications (Zhai 2009; Wu *et al.* 2017). Especially the timing of peak metamorphism of these granulites is highly contentious, and available data reveal two controversial peak metamorphic ages of ~1950–1900 Ma and ~1850–1800 Ma. For instance, some authors suggested that the metasedimentary rocks (named as khondalite series hereafter) and garnet-bearing mafic granulites were respectively formed at ~1950 Ma and ~1850 Ma in response to two independent orogens, namely the Khondalite Belt and Trans-North China Orogen (Zhao *et al.* 2005, 2008, 2010, 2012). In contrast, some authors suggested these granulites probably had similar metamorphic histories and petrogenesis, instead of representing different tectonic slabs with individual metamorphic histories (Zhai and Santosh 2011; Zhang *et al.* 2014; Wang *et al.* 2016; Wu *et al.* 2016, 2017; Zhou *et al.* 2017). Hence, clarifying whether or not these granulites have shared or separate metamorphic histories is one of the currently important issues.

Datong–Huai’an area is located at north-central part of the NCC, conjunction zone of the Fengzhen mobile belt and Jinyu mobile belt (Figure 1(a)), southern part of the Northern Hebei Orogen (Figure 1(b)), or the Inner Mongolia Suture Zone (Khondalite Belt) and Central Orogenic Belt (Trans-North China Orogen) (Figure 1 (c, d)). Varying Palaeoproterozoic granulite-facies rocks are broadly exposed and spatially associated, for example, in Manjinggou, western Hebei, Chicheng, northwestern Hebei, Huangtuyao, eastern Inner Mongolia, Gushan and Sifangdun, northern Shanxi provinces (Figure 2(a); Wu *et al.* 2017). It provides a suitable location to constrain the metamorphic histories and petrogenetic relations of these granulites from the north-central NCC. Recently, the identification of relict kyanite–garnet–K-feldspar-bearing assemblages in garnet porphyroblasts suggests that some pelitic granulites from the Huai’an complex underwent high-pressure (HP) granulite-facies conditions, in accordance with P - T results of the associated garnet-bearing mafic granulites (Wu *et al.* 2016, 2017). It induces us to consider that both types of granulites might share their metamorphic histories. Here, new zircon U–Pb ages from various granulite-facies rock associations from

Datong–Huai’an area are presented to better constrain the timing of granulite-facies metamorphism, and then to discuss their geological significance.

2. Major granulite-facies lithological associations

The Palaeoproterozoic granulite-facies rocks in the NCC are mainly comprised of three kinds of rock associations: (1) khondalite series (meta-sedimentary rocks), for example, metapelites (pelitic granulites); (2) metabasites, characterized by garnet-bearing mafic granulites; and (3) grey gneisses and associated charno-enderbitic gneisses (felsic granulites) (Zhai 1991, 1997). In the outcrops of Gushan and Manjinggou from Datong–Huai’an area, the above-mentioned granulite-facies lithologies are broadly exposed and spatially associated (Figure 2).

In Gushan area, there are three lithological domains from southeast to northwest: (1) the grey gneiss domain, (2) the transition zone between the khondalite series domain and grey gneiss domain, and (3) the widespread khondalite series domain (Figure 2(b); Wu 2016; Wu *et al.* 2017). In the second domain, garnet-bearing mafic granulites are closely associated with pelitic granulites and grey gneiss in spaces. In Manjinggou area, there are six lithological units from north to south: (1) the Shuigoukou grey gneiss, (2) the banded gneiss (intercalated tonalitic gneiss and mafic-to intermediate-granulite), (3) the garnet-bearing mafic granulite, (4) the khondalite series, (5) the Dongjiagou granitic gneiss, and (6) the Dapinggou garnet-bearing granite (Figure 2(c); Guo *et al.* 1993; Zhao *et al.* 2008, Zhao *et al.* 2010).

2.1 Grey gneiss (felsic granulite)

The grey gneiss in the Datong–Huai’an area is termed as the Huai’an TTG gneiss terrane, and mainly comprises of Archaean to Palaeoproterozoic dioritic, tonalitic, trondhjemitic, and granodioritic gneisses, with minor charno-enderbitic gneiss and potassic granitic gneiss (e.g. Guo *et al.* 1993; Zhao 1993; Zhang *et al.* 1994, 2011; Zhao *et al.* 2008; Santosh *et al.* 2013; Su *et al.* 2014). Some mafic enclaves are included in the grey gneiss, and they together formed banded gneiss. Besides, some isolated rafts of meta-supracrustal rocks, such as banded iron formations, are preserved in the grey gneiss (Zhao 1993; Zhang *et al.* 1994). Recent zircon U–Pb ages reveal that the grey gneiss mainly formed at 2550–2450 Ma and metamorphosed at 1950–1800 Ma (Zhao *et al.* 2008; Wang *et al.* 2010; Liu *et al.* 2012; Zhang *et al.* 2012a; Santosh *et al.* 2013; Wei *et al.* 2013; Su *et al.* 2014). Besides, some Palaeoproterozoic granitic gneisses

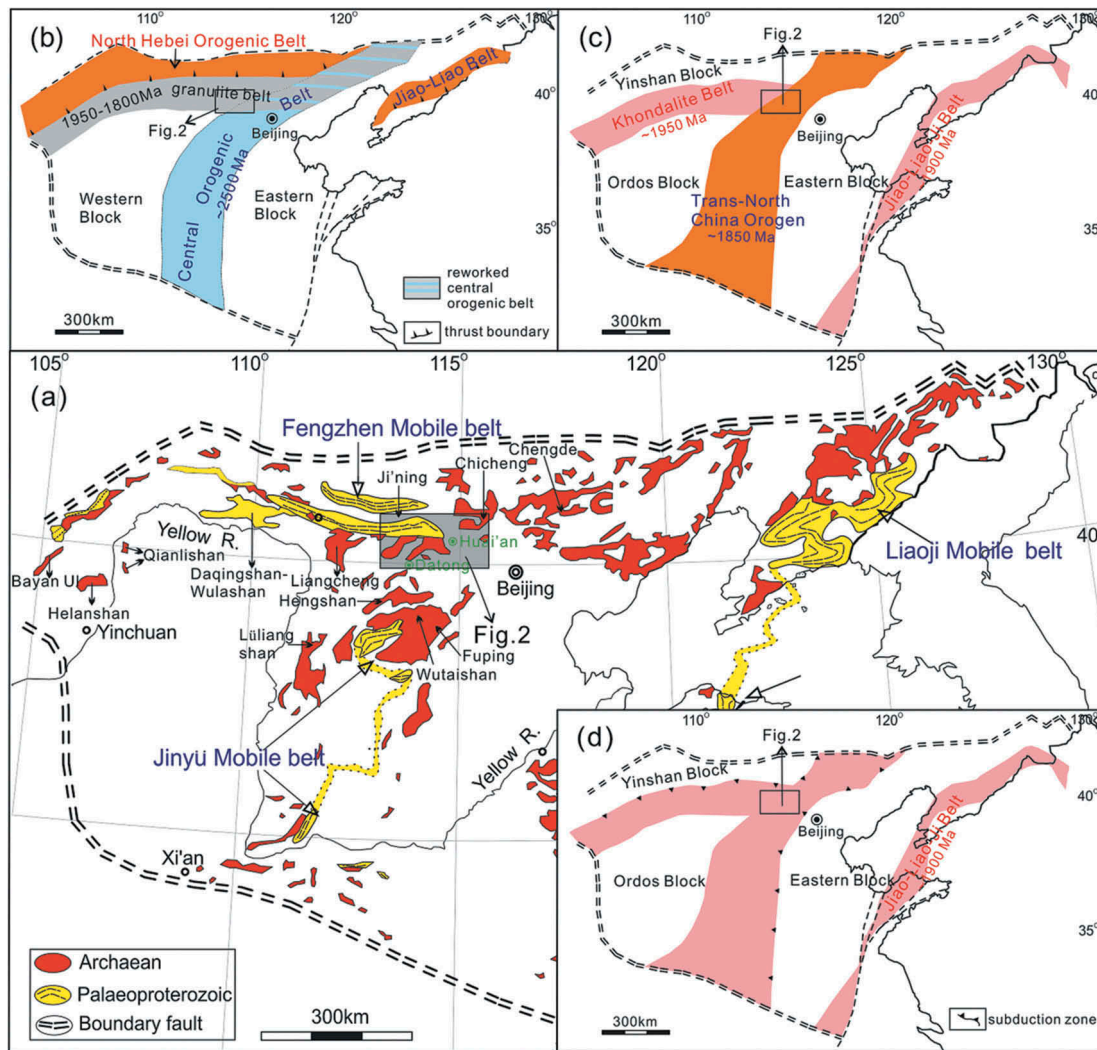


Figure 1. Tectonic subdivision of the NCC: (a) after Zhai and Santosh (2011), (b) after Kusky *et al.* (2007), (c) after Santosh *et al.* (2010), and (d) after Zhao *et al.* (2012).

intruded into the grey gneiss (Zhao *et al.* 2008; Zhang *et al.* 2011; Santosh *et al.* 2013; Su *et al.* 2014; Yang *et al.* 2014a; Wang *et al.* 2015).

2.2 Garnet-bearing mafic granulite (metabasite)

The early Proterozoic HP granulites from the NCC were firstly recognized in Huai'an–Hengshan area (Wang *et al.* 1991; Zhai *et al.* 1992). The HP rock associations mainly consist of garnet-bearing mafic granulites, with minor garnet pyroxenites and retrograde eclogites (Wang *et al.* 1991; Zhai *et al.* 1992, 1995; Guo *et al.* 1998, 2015; Zhao *et al.* 2001; Wu *et al.* 2018). We here use garnet-bearing mafic granulites to represent them. Field investigations reveal that the garnet-bearing mafic granulites mainly have two types of occurrence: (1) as lens or sill-like bodies within TTG gneiss and migmatic granitic gneiss (Guo *et al.* 1993, 2002; Zhang *et al.* 1994; Li *et al.* 1998), and (2) as lens or dismembered dikes in

the khondalite series (Wu *et al.* 1994, 2017; Li *et al.* 1998; Zhong 1999; Zhang *et al.* 2014; Wang *et al.* 2016).

The garnet-bearing mafic granulites are characterized by well-developed corona and symplectite of plagioclase and orthopyroxene around porphyroblastic garnet. The estimated peak metamorphic conditions are ~11–15 kbar/750–900°C, up to the transition zone of granulite-facies and eclogite-facies (Zhai *et al.* 1992, 1995; Zhao *et al.* 2001; Guo *et al.* 2002). The metamorphic ages of the garnet-bearing mafic granulites are still hotly debated. Some studies suggest that the peak metamorphic age is around ~1850 Ma (Mao *et al.* 1999; Guo and Zhai 2001; Guo *et al.* 2005; Kröner *et al.* 2006; Zhao *et al.* 2008; Wang *et al.* 2010; Xiao and Liu 2015), but others suggest ~1850 Ma represents retrograde age (Zhang *et al.* 2006, 2009, 2014, 2016a; Trap *et al.* 2011; Wang *et al.* 2011, 2015, 2016; Chu *et al.* 2012; Wei *et al.* 2014; Qian *et al.* 2017; Qian and Yin 2016; Wu *et al.* 2016; Wu 2016; Zhai 2009; Zhou *et al.* 2017).

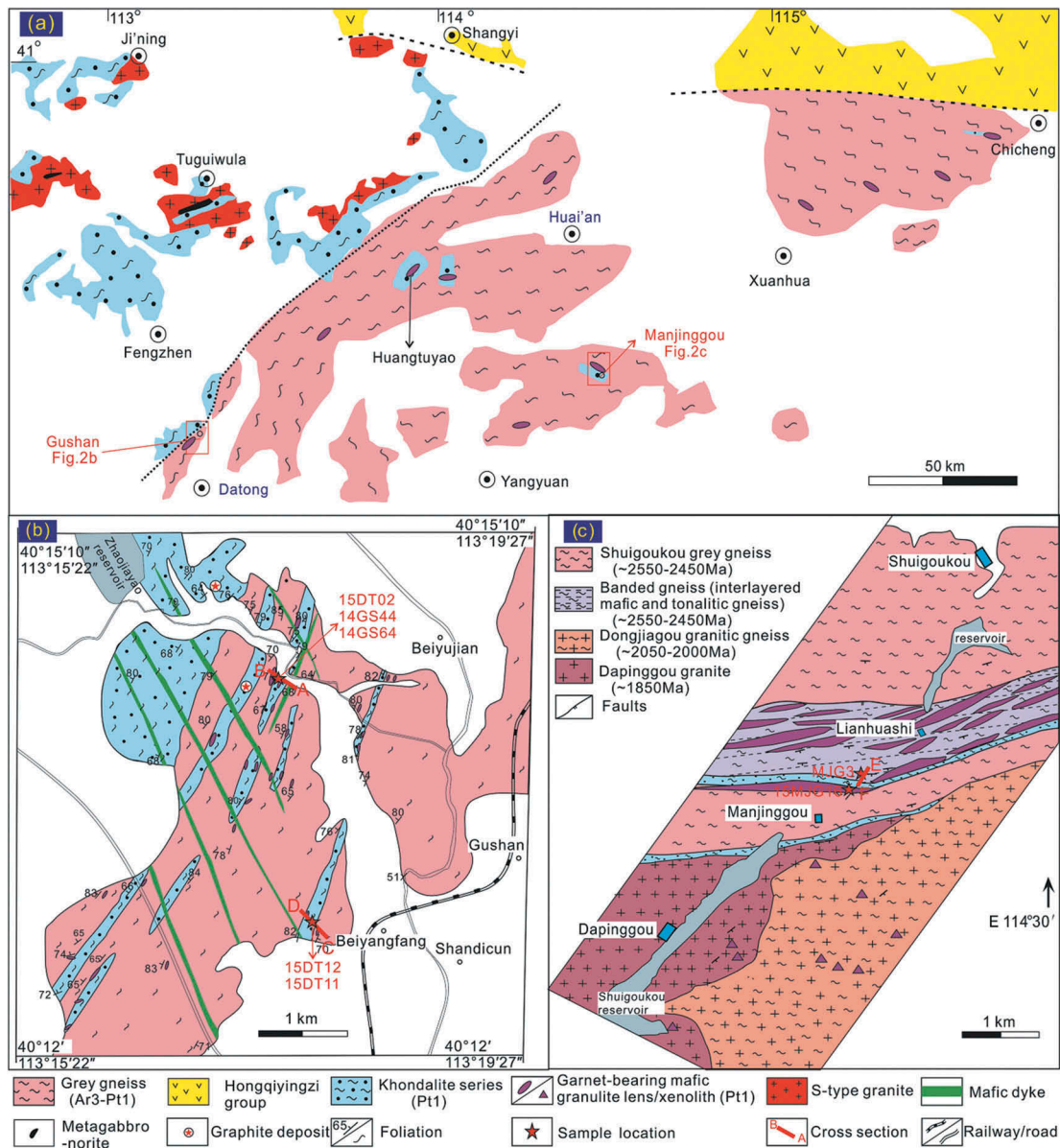


Figure 2. (a) Lithological map of Datong–Huai'an area, the north-central NCC, modified after Guo *et al.* (2002). (b) Geological map of Gushan area, Datong (Wu 2016). (c) Geological map of Manjinggou area, Huai'an (Guo *et al.* 1993).

2.3 Pelitic granulite (metasedimentary rock)

The pelitic granulites mainly consist of garnet, sillimanite, K-feldspar, plagioclase, quartz, biotite, sometimes with minor rutile, ilmenite, cordierite, sapphirine, spinel, and quartz, suggesting that they formed under HT to UHT conditions, and also termed as HT–UHT granulites (Zhai 2009). Some garnet- and cordierite-bearing S-type granites and minor metagabbro-norites are associated with these pelitic granulites (Figure 2(a); Lu *et al.* 1991, Lu *et al.* 1996; Peng *et al.*). In the study area, the pelitic granulites are mainly exposed in the Ji'ning area, with minor in the Datong–Huai'an area. Some authors proposed that the

HT–UHT pelitic granulites in the Ji'ning area marked a Palaeoproterozoic suture zone (Wu and Zhong 1998; Jin 2002; Zhao *et al.* 2005; Wu 2007; Santosh 2010), named as the Khondalite Belt (Zhao *et al.* 2005), or the Inner-Mongolia Suture Zone (Santosh 2010). However, the origin of the pelitic granulites from the Datong–Huai'an area, the north-central part of the NCC is still poorly constrained. For example, Zhao *et al.* (2005) assumed the pelitic granulites from Huai'an area represented tectonic nappes from the Khondalite Belt during assembly of the Eastern Block and Western Block at ~1850 Ma (Zhao *et al.* 2010). Wu and Zhong (1998) assumed that the protoliths of the pelitic granulites in the Huai'an and Ji'ning areas

were parts of the passive continental margin sediments of the Ordos Block, and metamorphosed during the SW–NE collision among the Ordos Block, Yinshan Block, and Eastern (Hebei–Shandong–He’nan) Block (Wu 2007).

The pelitic granulites were previously considered to be metamorphosed under intermediate- to low-pressure (IP–LP) granulite-facies conditions (e.g. Lu *et al.* 1991, 1996; Yan *et al.* 1991; Liu *et al.* 1992). Recent studies recognized that some pelitic granulites have experienced HP granulite-facies conditions (e.g. Ma and Wang 1995; Wu *et al.* 2016, 2017). For those sapphirine-bearing UHT granulites, the maximum of temperature was estimated around 900–1100°C, but their *P–T* paths are still controversial, that is, clockwise or counterclockwise (e.g. Liu *et al.* 2008; Santosh *et al.* 2009a, 2012; Tsunogae *et al.* 2011; Guo *et al.* 2012; Zhang *et al.* 2012b; Shimizu *et al.* 2013; Jiao *et al.* 2013a; Yang *et al.* 2014b; Li and Wei 2018). Available zircon ages demonstrate that their protoliths might be deposited at ~2000 Ma and metamorphosed during ~1950–1800 Ma (e.g. Wan *et al.* 2006, 2009; Xia *et al.* 2006, 2008; Yin *et al.* 2009, 2011; Zhao *et al.* 2010; Cai *et al.* 2015, 2017a; Wang *et al.* 2015).

3. Sampling and petrology

3.1 Sampling

Seven representative samples were collected from the Gushan and Manjinggou outcrops of Datong–Huai’an area. Five samples were selected from the Zhaojiayao reservoir (Figure 3(a)) and Beiyangfang (Figure 3(b)) cross sections in the Gushan outcrop. They include a tonalitic gneiss (15DT02), a charnockitic gneiss (14GS44), a garnet-bearing mafic granulite (15DT12), a two-pyroxene mafic granulite (15DT11), and a spinel-perthite–garnet granulite (14GS64) (Figures 3(a, b) and 4(a–f)). All of these rocks in both cross sections displayed concordant NNE to NE foliations (dip > 65°), with elongated sillimanite, biotite flakes in the pelitic granulites, and chain-like pyroxenes in the grey gneiss or charno-enderbitic gneiss. Locally, some orthopyroxene/amphibole–plagioclase symplectites around garnets are also oriented along the regional foliations.

A representative garnet-bearing mafic granulite (15MJG16) and a kyanite-bearing pelitic granulite (MJG3) were collected from the Manjinggou cross section (Figure 3(c)). It mainly comprises of the banded gneiss, with subordinate khondalite series, garnet-bearing mafic granulites, and potassic granitic gneiss (Figure 4(g–h)). All of these rock associations shared similar NEE–EW-trending foliations, featured by alignment of oriented sillimanite, biotite, quartz, and pyroxene in these rocks. All lithological units were truncated

or intruded by late pegmatitic granitic veins, such as the ~1812 million year hyalophane-rich pegmatite vein in this cross section (Qu *et al.* 2012).

3.2 Petrology

The tonalitic gneiss (15DT02) mainly consists of plagioclase (55–65%), quartz (15–20%), with minor orthopyroxene (5–10%) and clinopyroxene (1–3%) (Figure 5(a)). The charnockitic gneiss (14GS44) is mainly comprised of plagioclase (35–45%), K-feldspar (10–30%), quartz (10–25%), with a few orthopyroxene (5–10%), clinopyroxene (1–3%), and garnet (<1%) (Figure 5(b)). Geochemical data indicate that composition of the charnockitic gneiss in Gushan outcrop is quartz dioritic or granitic gneiss (Wang *et al.* 2015).

MJG3 is a coarse-grained kyanite-bearing pelitic granulite from Manjinggou area, with mineral assemblages of garnet, K-feldspar, kyanite, quartz, biotite, rutile, sillimanite, ilmenite and sporadic muscovite, and zinc spinel (Figure 5(c)). A detailed petrographical description refers to Wu *et al.* (2016). Four metamorphic generations were recognized in the pelitic granulite: the prograde (M_1), peak (M_2), decompression (M_3), and cooling (M_4) stages. M_1 is characterized by mineral inclusions within garnet core, including biotite + rutile + quartz ± muscovite ± plagioclase. M_2 is comprised of mineral assemblages of garnet mantle and its inclusions (kyanite + rutile + biotite + K-feldspar + quartz ± muscovite ± Zn spinel). M_3 consists of mineral assemblage of garnet outer rim + sillimanite + quartz + K-feldspar ± rutile ± ilmenite ± biotite ± Zn spinel. M_4 is featured by breakdown of garnet into biotite and quartz, with minor sillimanite and plagioclase. The estimated *P–T* conditions of M_1 to M_4 are ~10 kbar/~700°C, 11.5–15 kbar/810–860°C (up to 900°C), ~9.5 kbar/~850°C, ~5–7 kbar/~650°C (Wu *et al.* 2016).

The spinel-bearing granulites always occur as black stripes or layers within pelitic granulites in Gushan area (Wu 2016). The studied sample 14GS64 is a spinel–perthite–garnet granulite, occurring as ~10–30 cm layer between the calc-silicates and garnet-bearing mafic granulite. It is SiO₂ undersaturated, and its typical mineral assemblage consists of spinel (40–50%), perthite (20–30%), garnet (5–10%), and ilmenite (~5%), with minor plagioclase, biotite, corundum, and magnetite in local domains (Figure 5(d)). Rare sillimanite needles and quartz grains can only be detected in garnet porphyroblast but not in matrix, which suggest they probably represent earlier generation minerals. The exsolution volumes of plagioclase in perthite are in a range of 10–20%, and the estimated temperatures based on reintegrated compositions of former feldspar are ~870–890°C (Wu 2016).

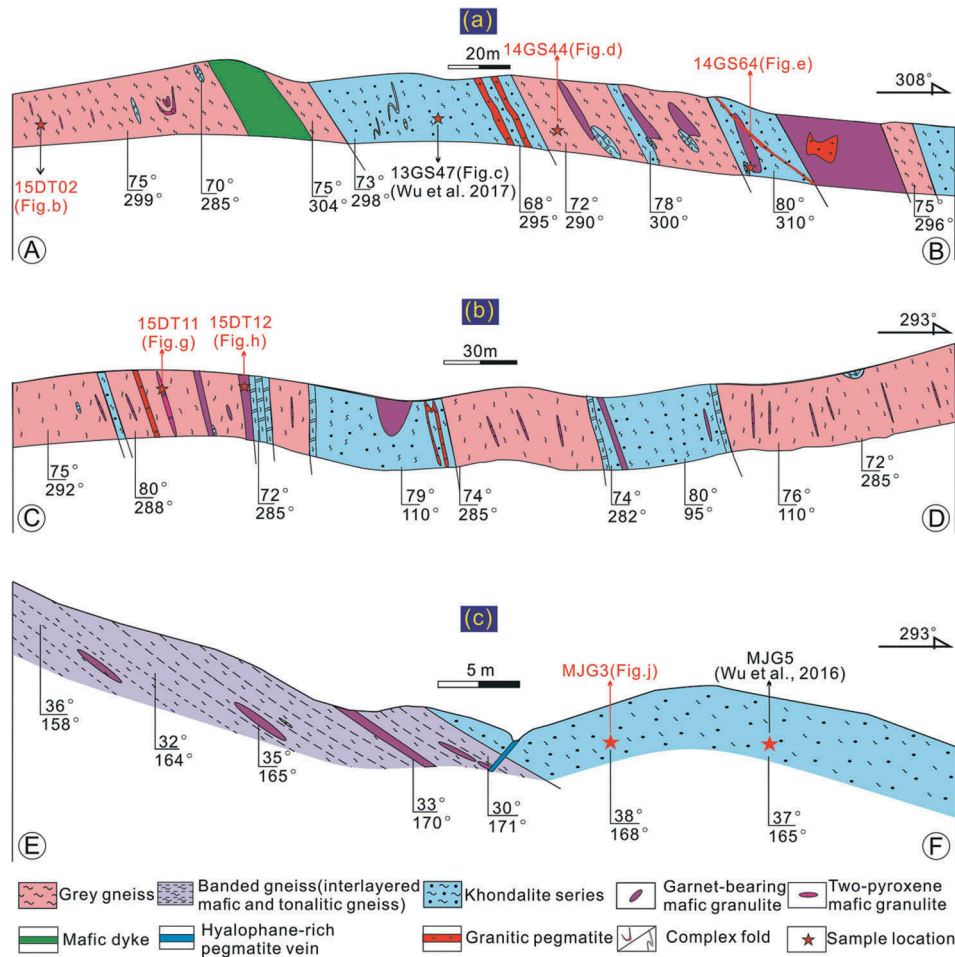


Figure 3. Cross sections from Datong–Huai’an area, shown in Figure 2(b, c). (a, b) Zhaojiayao reservoir and Beiyangfang cross sections, Datong (Wu 2016); (c) Manjinggou cross section, Huai’an (Wu *et al.* 2016).

15MJG16 and 15DT12 are coarse-grained garnet-bearing mafic granulites, and mainly consist of garnet, clinopyroxene, plagioclase, hornblende, with minor quartz, rutile, orthopyroxene, biotite, titanite, ilmenite, and magnetite (Figure 5(e–g)). The former (15MJG16) occurs as lens within tonalitic gneiss from Manjinggou outcrop, the latter (15DT12) occurs as dike intruded into the pelitic granulites in Gushan outcrop. The garnet grains from both samples develop corona of plagioclase + orthopyroxene, and kelyphites of plagioclase + amphibole. The cores of some garnet grains also breakdown to plagioclase and orthopyroxene (Figure 5(f)). Some clinopyroxene grains are replaced by amphibole (Figure 5(f, g)). Minor biotite flakes are adjacent to garnet, pyroxene, and amphibole (Figure 5(e, f)), representing retrograde products. Petrological studies revealed that the garnet-bearing mafic granulites in Datong–Huai’an area documented four generations of metamorphic assemblages from prograde (M_1), peak (M_2), decompression (M_3) to cooling (M_4) stages (Guo *et al.* 2002, 2015; Wu *et al.*

2018). M_1 is represented by mineral inclusions within garnet core, that is, clinopyroxene + quartz + rutile + plagioclase \pm titanite, representing metamorphic prograde assemblage. M_2 is characterized by a typical HP granulite-facies assemblage of garnet mantle + clinopyroxene + plagioclase + rutile \pm quartz, representing peak metamorphic assemblage. M_3 is featured by corona of orthopyroxene + plagioclase around porphyroblastic garnet. M_4 is represented by symplectites and kelyphites of amphibole + plagioclase around garnet. The estimated P – T conditions of M_1 to M_4 are ~ 10 kbar/700°C, 11–14.5 kbar/750–870°C, 8.5–10.5 kbar/770–830°C, and 5.5–8 kbar/500–600°C, respectively (Zhai *et al.* 1992; Zhang *et al.* 1994; Guo *et al.* 2002, 2015; Wu *et al.* 2018).

15DT11 is a two-pyroxene mafic granulite, occurring as mafic dike within grey gneiss. The mineralogy of the studied sample consists of plagioclase (40–50%), orthopyroxene (15–20%), clinopyroxene (15–20%), and amphibole (5–10%), with minor opaque minerals (ilmenite and/or magnetite) (Figure 5(h)).



Figure 4. Field photos of analysed samples. The onalitic gneiss (15DT02), enclosed some mafic enclaves (a), the kyanite-bearing HP pelitic granulite (13GS47) described in Wu *et al.* (2017) (b), the charnockitic gneiss-14GS44 (c), the spinel–perthite–garnet granulite-14GS64 (d), the two-pyroxene mafic granulite (15DT11) as dike in the grey gneiss (e), the garnet-bearing mafic granulite (15DT12) associated with pelitic granulites (f), kyanite-bearing pelitic granulite-MJG3 (g), and garnet-bearing mafic granulite (15MJG16) in the grey gneiss (h).

4. Analytical methods

Zircon grains were separated by conventional processes involving crushing, heavy liquid, magnetic separation, and then mounted in epoxy resin and polished. Both microscope and cathodoluminescence (CL) images

were taken to reveal their internal structures and determine suitable spot sites for U–Pb analyses. *In situ* U–Pb dating were performed using an Agilent 7500a ICPMS instrument with a 193-nm ArF excimer laser at the State Key Laboratory of Continental Dynamics, Northwest University, Xi’an, China. The laser spot diameter and

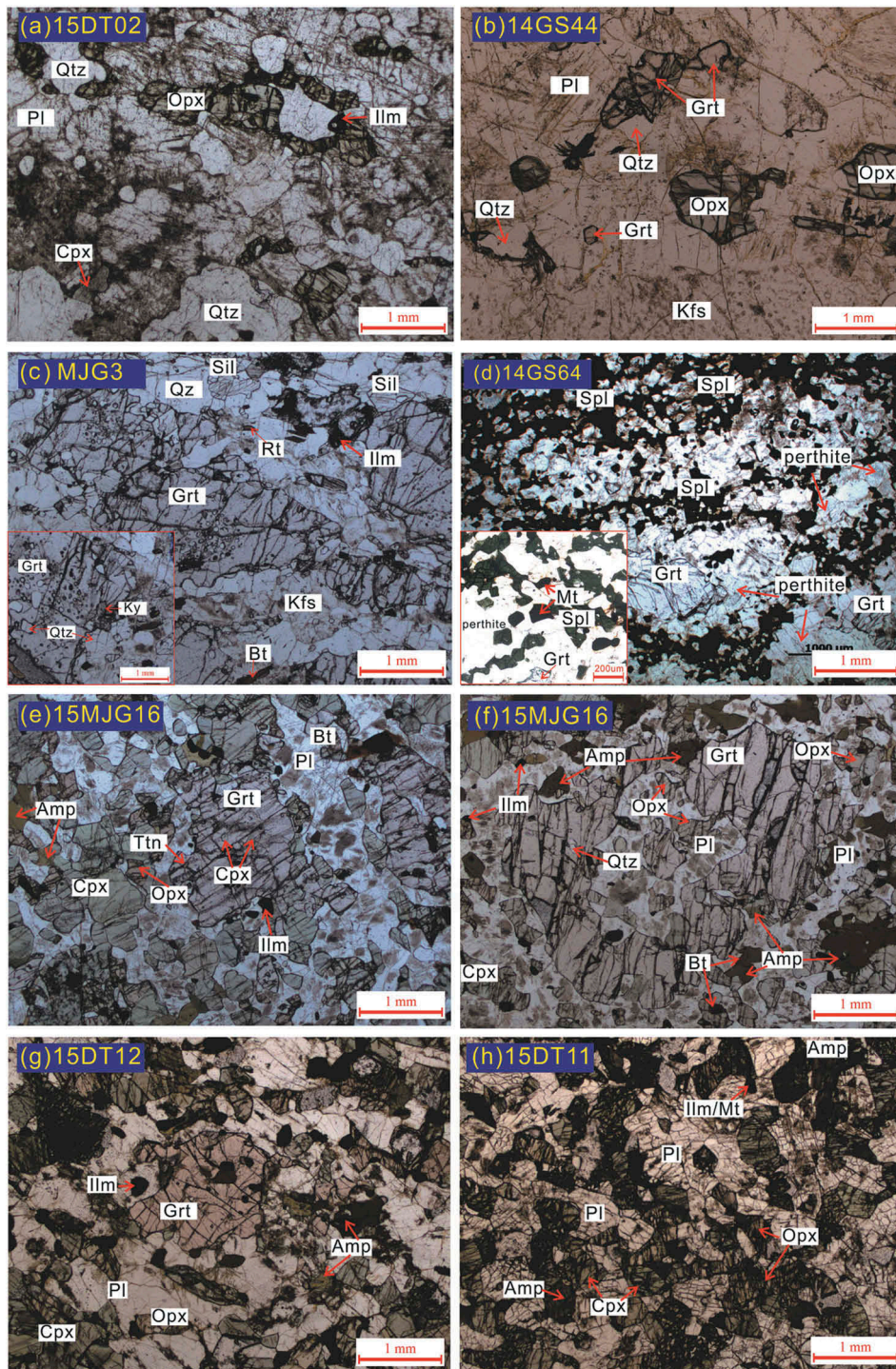


Figure 5. Representative photomicrographs of various granulite-facies rocks analysed in this study. (a) Tonalitic gneiss (15DT02), (b) charnockitic gneiss (14GS44), (c) kyanite-bearing pelitic granulite (MJG3), (d) spinel-perthite-garnet granulite (14GS64), (e, f) garnet-bearing mafic granulite (15MJG16), (g) garnet-bearing mafic granulite (15DT12), and (h) two-pyroxene mafic granulite (15DT11). Mineral abbreviations: Grt, garnet; Pl, plagioclase; Opx, orthopyroxene; Cpx, clinopyroxene; Qtz, quartz; Sil, sillimanite; Ky, kyanite; Kfs: K-feldspar; Bt: biotite; Amp: amphibole; Rt: rutile; Spl: spinel; Ilm: ilmenite; Mt: magnetite.

frequency were 30 μm and 6 Hz, respectively. Zircon 91500 was used as the standard, and the standard silicate glass NIST610 was employed to optimize the instrument. The trace element concentrations were

calibrated by using ^{29}Si as an internal standard and NIST610 as an external reference material. Raw data were processed using the GLITTER4.0 program to calculate isotopic ratios and ages of $^{207}\text{Pb}/^{206}\text{Pb}$, $^{206}\text{Pb}/^{238}\text{U}$,

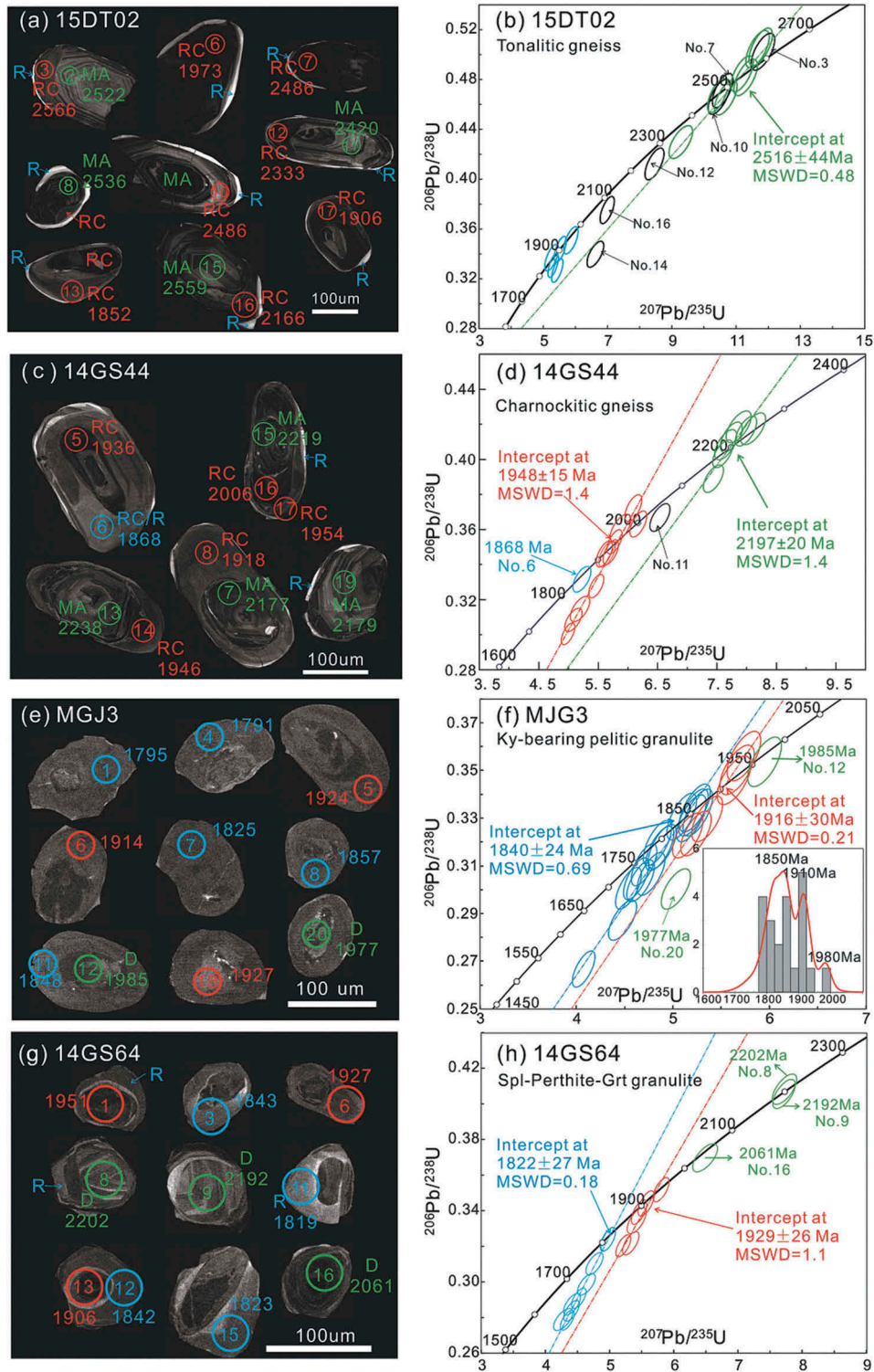


Figure 6. Representative CL images and concordia diagram of U–Pb analyses of zircons from the studied samples from Datong–Huai’an area.

and $^{207}\text{Pb}/^{235}\text{U}$. Common Pb was corrected according to the method of Anderson (2002), and the final ages were calculated by Isoplot program (Ludwig 2012). All of the zircon U–Pb data and trace element contents are listed in Supplementary Table 1.

5. Results

5.1 Sample 15DT02 (tonalitic gneiss)

The zircons from this sample display prismatic to sub-hedral shapes, with size of 100–200 µm. Most of the

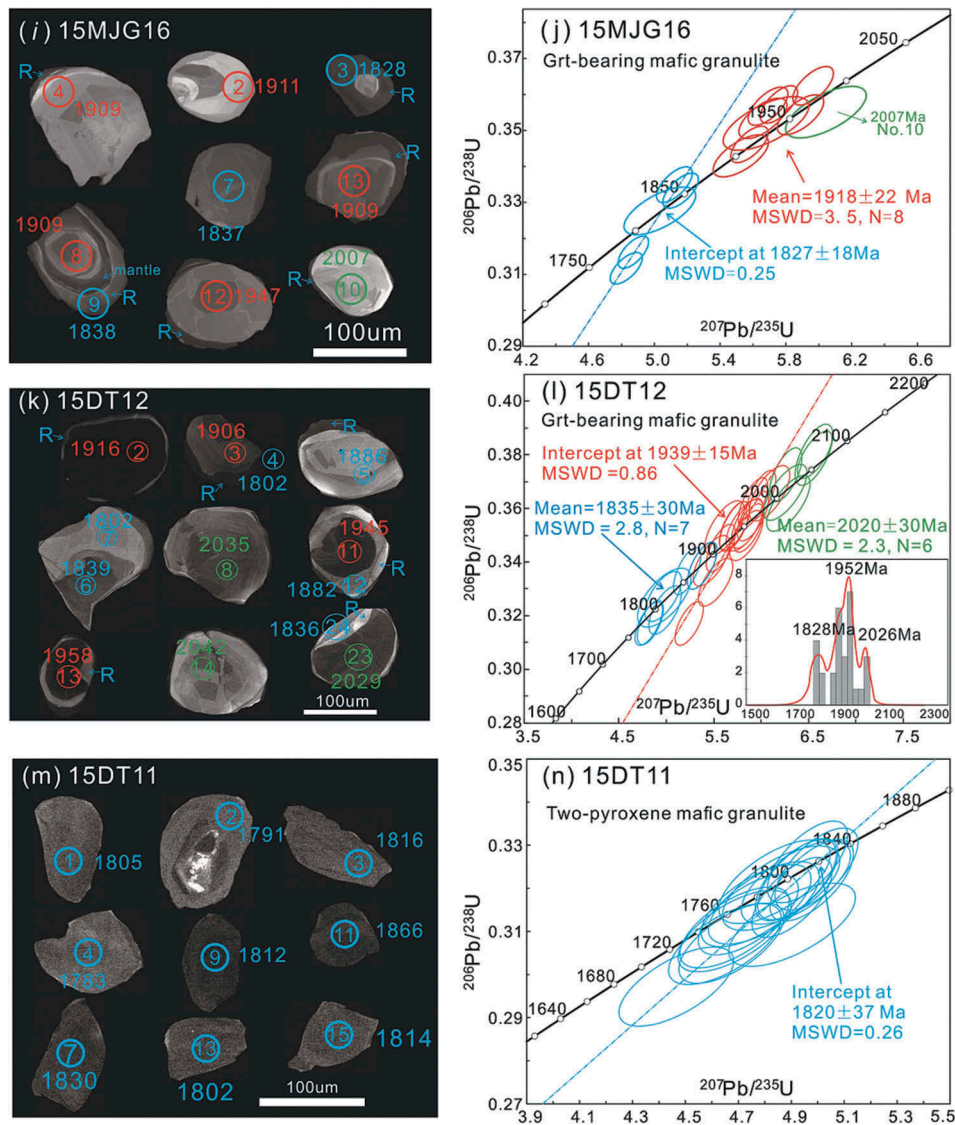


Figure 6. Continued.

zircon grains exhibit typical magmatic oscillatory zoning in the cores and recrystallized or overgrown rims with variable thicknesses in the CL images. The magmatic cores have Th, U contents in the range of 29–105, 62–213 ppm, with relatively homogeneous Th/U ratios of 0.32–0.67. Seven analyses on the magmatic cores yield an upper intercept age of 2516 ± 44 Ma (MSWD = 0.48). The recrystallized domains exhibit variable Th, U contents and Th/U ratios of 19–283, 41–316 ppm and 0.10–6.56 (Figure 7(h)). The $^{207}\text{Pb}/^{206}\text{Pb}$ ages range from 1852 to 2566 Ma, which can be divided into three groups: 2486–2566 Ma (nos. 3, 7, and 10), 2166–2333 Ma (nos. 12, 14, and 16), and 1852–1973 Ma (four analyses) (Figure 6(b)). The former (~2500 Ma) can compare with regional tectono-thermal event at Archaean–Palaeoproterozoic boundary (e.g. Kröner *et al.* 1998; Liu *et al.* 2011), the last group

(~1850–1950 Ma) can correspond to the late Palaeoproterozoic metamorphism in the NCC (e.g. Zhao *et al.* 2008; Liu *et al.* 2012; Santosh *et al.* 2013; Wang *et al.* 2015). However, the middle group ages (2166–2333 Ma) document strong lead loss, which might be meaningless and result from resetting of the U–Pb system of the magmatic zircons. No U–Pb data were analysed on the bright rims due to their very thin thickness. Correspondingly, the four group domains display different rare earth element (REE) patterns in Figure 7(a). The magmatic cores display steep heavy rare earth element (HREE) patterns. The recrystallized zircon domains display decreasing content of HREE, the younger ages, the lesser of HREE, similar to the results of Luo *et al.* (2012). For example, the HREE of zircon domain (1852 ± 22 Ma, 1δ) exhibits flat to relatively negative pattern from Gd to Lu.

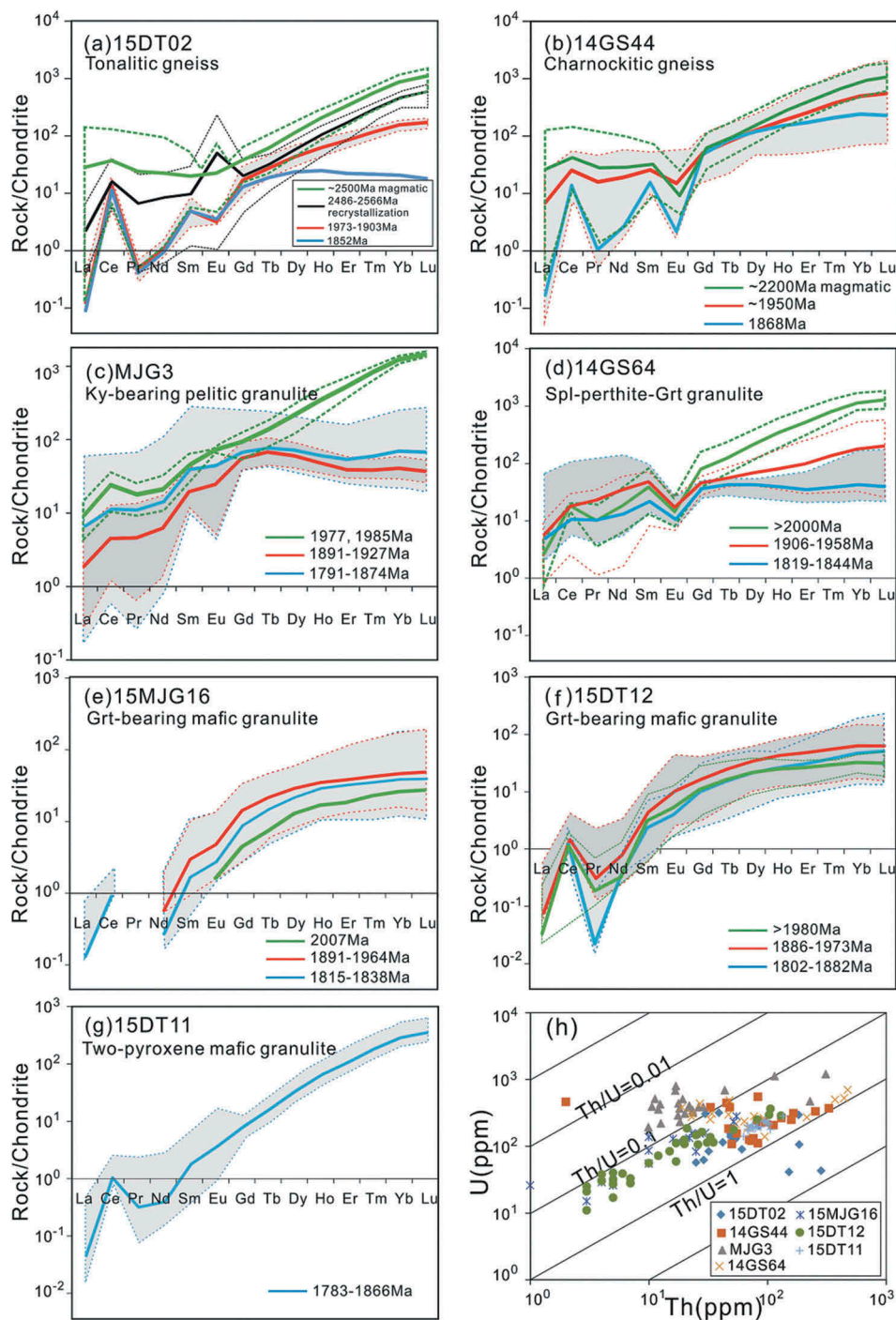


Figure 7. Chondrite-normalized REE patterns of zircons in samples from Datong–Huai'an area. The normalization values of chondrite are from Sun and McDonough (1989). The solid lines represent average values of different age populations from distinct zircon domains: green line: magmatic or detrital zircon domains; red line: zircon domains with the older metamorphic ages (~1970–1900 Ma); blue line: zircon domains with the younger metamorphic ages (<1900 Ma).

5.2 Sample 14GS44 (charnockitic gneiss)

The zircons from this sample range in size from 120 to 200 μm , and are elongate, prismatic, to stubby. Most of the zircons exhibit regular core-and-rim structures with

magmatic cores and relatively thick metamorphic rims (Figure 6(c)). Twenty spots were analysed on 13 zircon grains. Seven analyses on the magmatic cores (except no. 11) yield an upper intercept age of 2197 ± 20 Ma (MSWD = 1.4), with Th, U contents and Th/U ratios

ranging from 55–329, 121–368 ppm and 0.35–0.89. Eleven analyses on the recrystallized domains yield an upper intercept age of 1948 ± 15 Ma (MSWD = 1.4). One analysis (no. 6) yields a concordant age of 1868 ± 16 Ma (1 δ) (Figure 6(d)). The Th, U contents and Th/U ratios of these domains are in the range of 2–131, 108–550 ppm and 0–0.75 (Figure 7(h)). The recrystallized domains have lower content of HREE than the magmatic domains, similar to those of the sample 15DT02.

5.3 Sample MJG3 (kyanite-bearing pelitic granulite)

The zircons from this sample are mostly subrounded, stubby to weakly elongate in shape, with diameter ranging from 50 to 120 μm . Also, 24 spots were performed on 21 grains. Most zircons display low luminescence, with dark to grey cores and grey rims, or structureless in CL images, indicating a metamorphic origin (Figure 6(e)). Twenty-one spots were conducted on this type of zircon grains. The zircons have Th and U contents in range of 10–44 and 193–689 ppm, with Th/U ratios of 0.02–0.08 (Figure 7(h)). They have a range of $^{207}\text{Pb}/^{206}\text{Pb}$ ages from 1791 to 1927 Ma. The ages in the concordia diagram can be divided into two clusters with upper intercept ages of 1916 ± 30 Ma (MSWD = 0.21) and 1840 ± 24 Ma (MSWD = 0.69), corresponding to two discrete age peaks on the histogram, respectively (Figure 6(f)). The chondrite-normalized REE patterns of such zircon domains display flat to negative HREE (Figure 7(c)), suggesting their concurrent growth with garnet (e.g. Rubbato, 2002).

A few zircon cores are irregular or prismatic in shape and sometimes exhibit blur zoning, indicating an earlier generation, which might be origin of detrital, magmatic, or metamorphic grains (Figure 6(e)). Three spots (nos. 12, 16, and 20) were analysed on these types of zircons. They display high contents of Th, U and Th/U ratios in the range of 115–229, 471–1204 ppm and 0.1–0.49 (Figure 7(h)), and steep HREE patterns, contrasting with the above-mentioned metamorphic domains (Figure 7(c)). The $^{207}\text{Pb}/^{206}\text{Pb}$ ages of nos. 12 and 20 are 1985 ± 16 Ma (1 δ) and 1977 ± 50 Ma (1 δ), which might represent the detrital ages of sediment source, and suggest deposit time of their protoliths is possibly younger than ~1980 Ma. Alternatively, the results might represent prograde metamorphic ages, and their steep HREE patterns may represent recrystallized primitive magmatic grains under garnet-absent conditions. The spot (no. 16) yields a $^{207}\text{Pb}/^{206}\text{Pb}$ age of 1924 ± 55 Ma (1 δ), which is consistent with the older group

metamorphic ages, and might represent a resetting or mixing age, rather than a detrital age.

5.4 Sample 14GS64 (spinel-perthite-garnet granulite)

The zircons grains from this sample display subrounded shape and range in size of 50 to 120 μm . In CL images, many grains exhibit clear core-and-rim textures with grey to dark cores of variable shapes and grey rims of variable thicknesses. A few zircon cores have ambiguous magmatic features, mantled by structureless rims (Figure 6(g), nos. 8 and 9). Eighteen spots were analysed on 17 grains. The zircons have Th and U contents in range of 23–475 and 139–695 ppm, with variable Th/U ratios of 0.05–0.85 (Figure 7(h)). Among them, six spots on the metamorphic zircon cores display discordant $^{207}\text{Pb}/^{206}\text{Pb}$ ages, and yield an upper intercept age of 1929 ± 26 Ma (MSWD = 1.1), and another nine spots on the zircon rims yield an upper intercept age of 1822 ± 27 Ma (MSWD = 0.18). Three spots on detrital cores yield $^{207}\text{Pb}/^{206}\text{Pb}$ ages of 2016, 2192, and 2202 Ma (Figure 6(h)). In the chondrite-normalized REE diagram, the detrital zircon domains have steep HREE patterns, while the metamorphic domains have relatively flat patterns (Figure 7(d)).

5.5 Sample 15MJG16 (garnet-bearing mafic granulite)

The zircons in this sample display rounded to subrounded shapes in size of 80–150 μm . Most zircons show sector zoning, and a few grains exhibit core-and-rim structures (Figure 6(i)). Fifteen analyses were performed on 13 grains. The zircons have Th, U contents in range of 1–55, 15–280 ppm. The Th/U ratios range from 0.05 to 0.3, with most ratios >0.10 (Figure 7(h)). Eight analyses on zircons cores yield a weighted average $^{207}\text{Pb}/^{206}\text{Pb}$ age of 1918 ± 22 Ma (MSWD = 3.5). Five analyses on zircon rims yield an upper intercept age of 1827 ± 18 Ma (MSWD = 0.25). One analysis yields a weakly discordant age of 2007 ± 13 Ma (1 δ) (Figure 6(j)). No significant difference exists in the REE diagram of different zircon domains (Figure 7(e)).

5.6 Sample 15DT12 (garnet-bearing mafic granulite)

The zircons in this sample are spherical to oval in size of 80–150 μm . Many zircon grains exhibit two layers in CL images. The central regions are surrounded by light to grey rims with various thicknesses. Thirty-one analyses were performed on 20 grains. The zircons have Th, U

contents and Th/U ratios in range of 4–130, 11–361 ppm and 0.09–0.45 (Figure 7(h)). Most of the analyses yield concordant to weakly discordant ages in the range of 1790–2040 Ma, with the exception of a few discordant analyses, such as nos. 17, 20, and 22 (Supplementary Table 1). Six analyses on the grey cores with weakly magmatic-like oscillatory zoning yield a weighted average $^{207}\text{Pb}/^{206}\text{Pb}$ age of 2020 ± 30 Ma (MSWD = 2.3). Fourteen analyses on the dark and structureless cores yield an upper intercept age of 1939 ± 15 Ma (MSWD = 0.86). Seven analyses on the grey rims yield a weighted average $^{207}\text{Pb}/^{206}\text{Pb}$ age of 1835 ± 30 Ma (MSWD = 2.8). The three group ages correspond well to the three age peaks on the histogram (Figure 6(l)). The REE patterns of different zircon domains are similar (Figure 7(f)).

5.7 Sample 15DT11 (two-pyroxene mafic granulite)

The zircons from this sample range in size from 40 to 90 μm and show elongated to oval shapes. Most zircons show low luminescence and structureless in CL images with very few exceptions (Figure 6(m)). Eighteen analyses were conducted on 18 grains. The zircons have Th, U contents and Th/U ratios in limited ranges of 63–136, 140–281 ppm and 0.34–0.60 (Figure 7(h)). They display steep HREE patterns in chondrite-normalized REE diagram (Figure 7(g)). All the analyses yield concordant to

weakly discordant ages, with an upper intercept age of 1820 ± 37 Ma (MSWD = 0.26) (Figure 6(n)).

6. Discussion

6.1 Petrological records response to multistage metamorphic evolution

P–*T* evolution of the varying granulite-facies rock associations from the north-central NCC were considered to be diverse in early studies. The khondalite series were considered to be metamorphosed under *IP*–*LP* and *HT*–*UHT* granulite-facies conditions due to ubiquitous sillimanite- and cordierite-bearing assemblages in matrix (e.g. Yan *et al.* 1991; Liu *et al.* 1992; Lu *et al.* 1996; Santosh *et al.* 2012). The garnet-bearing mafic granulites and their surrounding grey gneiss mutually suffered *IP*–*HP* granulite-facies metamorphism (e.g. Zhai *et al.* 1992; Guo *et al.* 2002, 2015; O'Brein *et al.*, 2005; Kröner *et al.* 2006).

Recently, we noticed that garnet porphyroblasts in pelitic granulites from Datong–Huai'an area document abundant mineral inclusions, different from the matrix minerals, which mainly consist of garnet–sillimanite \pm cordierite-bearing assemblages (e.g. Lu *et al.* 1991; Yan *et al.* 1991; Liu *et al.* 1992). The identification of inclusion-type kyanite–garnet–K-feldspar-bearing assemblages in garnet indicates the pelitic granulites have ever experienced *HP* granulite-facies metamorphism before the extensive *IP*–*LP* granulite-facies overprint.

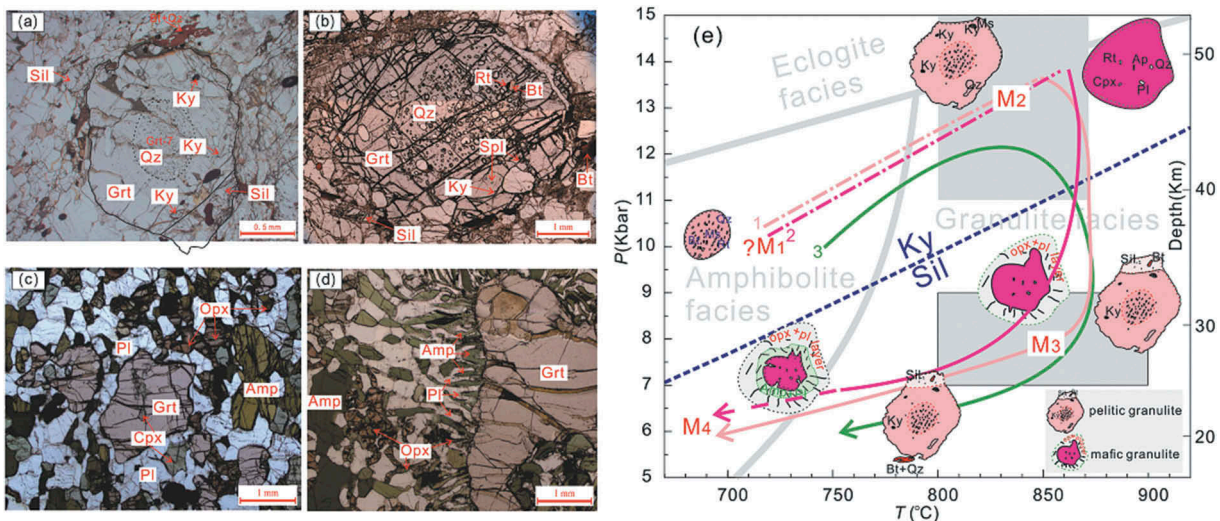


Figure 8. (a–d) Typical microphotographs of pelitic and mafic granulites from Datong–Huai'an area. (b) Selected *P*–*T* paths of the pelitic and mafic granulites from Datong–Huai'an area, and schematic model for garnet growth and resorption of both granulites along the *P*–*T* loops. 1: Mafic granulites from Huai'an area, modified after Guo *et al.* (2002) and Zhai *et al.* (1992). 2: Pelitic granulites in Manjinggou, Huai'an, after Wu *et al.* (2016). 3: Pelitic granulites in Gushan, Datong, after Wu *et al.* (2017).

Hence, the presently preserved sillimanite-type granulite-facies assemblages represent decompressed products of early kyanite-bearing HP granulites (Figure 8(a, b, e)). Using phase equilibrium modelling methods, Wu *et al.* (2016, 2017) estimated the peak metamorphic conditions of these pelitic granulites are 12 ± 2 kbar/ $850 \pm 50^\circ\text{C}$, consistent with those of the associated garnet-bearing mafic granulites.

Also, both types of granulites record comparable retrograde microstructures in response to variations of metamorphic conditions during exhumation (Figure 8). For the pelitic granulites (Figure 8(a, b)), kyanite is firstly transformed into sillimanite and rutile is also replaced by ilmenite during decompression. Then garnet begins to breakdown into biotite and quartz, with minor sillimanite and plagioclase during the cooling process (Wu *et al.* 2016, 2017). Comparably, garnet grains from the mafic granulites often exhibit well-developed corona/symplectites in response to retrogression (Figure 8(c, d); Zhai *et al.* 1992; Guo *et al.* 2002). For instance, some garnet grains may have two corona/symplectite layers, with an inner amphibole–plagioclase (Amp-Pl) layer separating an orthopyroxene–plagioclase (Opx-Pl) layer from the wrapped garnet (Figure 8(d, e)). It suggests that the P – T vector involved in the mafic granulites has sequentially crossed the reaction lines of garnet breakdown into Opx + Pl and then to Amp + Pl in P – T space (Wu *et al.* 2018). The microstructures and corresponding mineral compositions respectively documented a typical near isothermal decompression and a near isobaric cooling P – T segment from peak metamorphic to retrograde stages, which together define clockwise P – T loops for both granulites (Figure 8(e)). Additionally, recently structural analyses also suggest that the varying granulites shared similar Palaeoproterozoic deformation characteristics (e.g. Zhang *et al.* 2009, 2014). It induces us to consider that the various granulites from the study area should have similar metamorphic P – T histories at least since peak metamorphic stage (Figure 7(e); Zhang *et al.* 2014, Zhang *et al.* 2016a; Wang *et al.* 2016; Wu *et al.* 2016, Wu *et al.* 2017, Wu *et al.* 2018). Zircon U–Pb data on these granulites are discussed in the following section to test whether they were metamorphosed during one or two metamorphic cycles.

6.2 Interpretations of metamorphic ages from this study

The internal structures of zircon grains from seven investigated samples from Datong–Huai'an area suggest strong recrystallization and overgrowth under granulite-facies conditions (e.g. Vavra *et al.* 1999; Hoskin and Black

2000; Corfu *et al.* 2003). For the pelitic granulite (MJG3) and spinel–perthite–garnet granulite (14GS64), some zircons develop core-and-rim structures, with dark to grey cores and grey to light rims, or structureless. A few zircon grains preserve prismatic or oval cores with ambiguous magmatic oscillatory zoning, and are mantled by structureless rims. The structures are consistent well with those zircon grains in pelitic granulites from Manjinggou in Zhao *et al.* (2010), where they divided zircons into three types: (1) spherical grains without internal structures, (2) grains with core-and-rim structures, and (3) grains with a dark core surrounded by double rims. Besides, Liu *et al.* (2002) identified that mineral inclusions in zircons from pelitic granulites in Liangcheng, Inner Mongolia, can be divided into three type assemblages: (1) kyanite-absent mineral assemblages, (2) kyanite-bearing mineral assemblages, and (3) relict or inherited cores mantled by sillimanite- and garnet-bearing assemblages. They also recognized the mineral inclusion types and distribution patterns agree well with internal structures in CL images (Liu *et al.* 2002). For instance, in the type 2 zircons, mineral inclusion assemblages display a regular core-and-rim structure, that is, kyanite–K-feldspar–quartz \pm garnet \pm apatite in the cores, and sillimanite–garnet–K-feldspar–quartz \pm apatite in the rims. In type 1 and the rim of type 3 zircons, the mineral inclusions are similar as those of the rims of type 2. These features are also consistent with mineral inclusions currently preserved in garnets, in which kyanite–K-feldspar-bearing assemblages are included in the mantle or inner rims of garnet, representing HP granulite-facies assemblages, and sillimanite-bearing assemblages are in the outer rims of garnet, representing IP–LP granulite-facies assemblages (Figure 8(a, b, e); Wu *et al.* 2016, Wu *et al.* 2017).

In this study, the metamorphic zircon cores from kyanite-bearing pelitic granulites (MJG3) and spinel–perthite–garnet granulite (14GS64) respectively yield upper intercept ages of 1916 ± 30 Ma and 1929 ± 26 Ma, comparable with the results from the cores of type 2 and inner rims of type 3 (~ 1950 Ma) from two samples in Zhao *et al.* (2010). The metamorphic rims of MJG3 and 14GS64 respectively yield upper intercept ages of 1840 ± 24 Ma and 1822 ± 27 Ma, similar to the results from type 1, rims of type 2, and the outer rims of type 3 zircons (~ 1850 Ma) in Zhao *et al.* (2010). In this context, we intend to take the 1916 ± 30 Ma and 1929 ± 26 Ma (metamorphic cores' ages) to approximate the timing of HP granulite-facies metamorphism, and the 1840 ± 24 Ma and 1822 ± 27 Ma (metamorphic rims' ages) to represent the timing of IP–LP granulite-facies stages (e.g. Yin *et al.* 2011, 2014, 2015; Zhang *et al.* 2016a; Wu *et al.* 2017). Additionally, a few zircon cores yield concordant age of >2000 Ma, which

might represent detrital ages of source rocks (e.g. Xia *et al.* 2006, 2008; Yin *et al.* 2009, 2011; Hu *et al.* 2013; Cai *et al.* 2015, 2017a).

It was considered that garnet-bearing mafic granulites from the NCC were metamorphosed at ~1850 Ma in previous studies (Mao *et al.* 1999; Guo and Zhai 2001; Guo *et al.* 2005; Kröner *et al.* 2006; Zhao *et al.* 2008; Wang *et al.* 2010; Xiao and Liu 2015). For example, in Manjinggou, Huai'an area – the first locality for reporting of early Precambrian HP granulite terrane in the NCC, the peak metamorphic ages of garnet-bearing mafic granulites were thought to be around ~1870–1800 Ma (Guo *et al.* 2005; Zhao *et al.* 2008; Wang *et al.* 2010). However, recent analyses reveal that garnet-bearing mafic granulites from the north-central NCC also record metamorphic ages of ~1960–1900 Ma (e.g. Wang *et al.* 2011, 2016; Zhang *et al.* 2014, 2016a; 2016b; Tang *et al.* 2017; Qian *et al.* 2017; Table 1). We here select two garnet-bearing mafic granulites (15MJG16 and 15DT12) from Manjinggou and Gushan outcrops as examples to clarify their metamorphic chronology. Most zircon grains from the two samples are spherical to oval, with structureless, fir-tree zoning, sector zoning, or core-and-rim structures, and flat to negative HREE patterns, indicating their metamorphic origin (e.g. Vavra *et al.* 1999; Rubatto 2002; Corfu *et al.* 2003). Analyses on the metamorphic cores or part of the sector zoning domains yield a weighted mean $^{207}\text{Pb}/^{206}\text{Pb}$ age of 1918 ± 22 Ma (15MJG16) and an upper intercept age of 1935 ± 15 Ma (15DT12), while the rims yield an upper intercept age of 1827 ± 18 Ma (15MJG16) and a weighted mean age of 1835 ± 30 Ma (15DT12), respectively. The results are also consistent with recent studies of garnet-bearing mafic granulites and retrograde eclogites from Chicheng–Huai'an–Xuanhua–Tianzhen, northern Hengshan and Fuping area, the conjunction zone of Inner Mongolia–Hebei–Shanxi provinces (Zhang *et al.* 2014, 2016a, 2016b; Tang *et al.* 2017; Qian *et al.* 2017; Table 1). Zhang *et al.* (2016a) conducted detailed mineral inclusion studies in zircons from garnet-bearing mafic granulites in the Huai'an Complex and found that mineral inclusions in zircon domains of 1900–1800 Ma mainly include clinopyroxene, plagioclase, apatite, and titanite, and mineral compositions of the plagioclase and clinopyroxene are similar to those of retrograde stages. Hence, we intend to interpret the older population metamorphic ages of 1918 ± 20 Ma and 1935 ± 15 Ma to approximate the timing of HP granulite-facies metamorphism, and the younger population ages of 1827 ± 18 Ma and 1835 ± 30 Ma, comparable with the metamorphic ages of the two-

pyroxene mafic granulite (1820 ± 37 Ma), to represent the timing of IP–LP granulite-facies metamorphism.

Zircons from surrounding rocks (gneissic granitoids – TTG gneiss and granitic gneiss) of pelitic and mafic granulites also document strong Palaeoproterozoic recrystallization. The dark to grey and structureless zircon domains in the Neoproterozoic tonalitic gneiss (15DT02, 2516 ± 44 Ma) yield $^{207}\text{Pb}/^{206}\text{Pb}$ ages in the range of 1973–1852 Ma. A trondhjemitic gneiss (M19) from Manjinggou outcrop in Zhao *et al.* (2008) yielded similar age patterns – their magmatic cores yielded a weighted $^{207}\text{Pb}/^{206}\text{Pb}$ age of 2499 ± 19 Ma, and the rims yielded two group metamorphic ages of 1954 ± 32 Ma and 1838 ± 35 Ma (Zhao *et al.* 2008; see their Figure 8). Also, zircons from the Palaeoproterozoic charnockitic gneiss (14GS44, 2197 ± 20 Ma) document strong metamorphic features, with magmatic cores mantled by thick, grey, and structureless rims, which yield an upper intercept age of 1951 ± 16 Ma and one $^{207}\text{Pb}/^{206}\text{Pb}$ age of 1868 ± 16 Ma (1 δ). It agrees well with published metamorphic ages on the Neoproterozoic to Palaeoproterozoic gneissic granitoids in the northern NCC (Table 1; e.g. Ma *et al.* 2012; Liu *et al.* 2012; Luo *et al.* 2012; Zhao *et al.* 2008; Santosh *et al.* 2013; Zhang *et al.* 2013a, 2013b; Xu *et al.* 2015).

Figure 9 is a histogram of the zircon U–Pb ages of this study, which indicate that the varying granulite-facies lithologies from Datong–Huai'an area have mutually involved in the intensive and extensive Palaeoproterozoic (~1970–1790 Ma) metamorphism, although their protolith ages are contrasting from Neoproterozoic to Palaeoproterozoic. The metamorphic ages can be roughly divided into two clusters of ~1970–1900 Ma and ~1880–1790 Ma, culminating at ~1916–1938 Ma and ~1827 Ma, respectively (inset of Figure 9). The results agree well with regional metamorphic ages of various granulites from the northern part of the NCC (Table 1). In this regard, we suggest that the timing of HP granulite-facies metamorphism is at ~1916–1938 Ma, and the timing of IP–LP granulite-facies metamorphism is at ~1830 Ma.

6.3 Implication for petrogenetic relations of the varying granulites from the study area

Various tectonic interpretations were proposed on petrogenetic relations of the varying and spatially associated granulite-facies rocks from Datong–Huai'an area in early studies. For example, these granulites were interpreted as juxtaposed together by a tectonic mélange zone (Guo *et al.* 1993; Wang *et al.* 2015), or different crustal levels juxtaposed by late tectonic

Table 1. Summary of late Palaeoproterozoic metamorphic ages from various granulite-facies lithologies in the northern NCC.

Area	Rock	Metamorphic age	Reference
Gneissic Granitoid			
Byan Ul-Helanshan	Palaeoproterozoic gneissic granite	1923±28 Ma; 1856±12 Ma.	Dong et al., 2007
Daqingshan	Neoarchaeal-Palaeoproterozoic TTG gneisses; Palaeoproterozoic granitic gneiss	~1960-1840 Ma; 1845±10 Ma; 1970-1940 Ma; 1870-1820 Ma.	Ma et al., 2012; Liu et al., 2013a; Xu et al., 2015
Wulashan	Neoarchaeal-Palaeoproterozoic granitic gneiss	1936±20 Ma; 1894±39 Ma.	Liu et al., 2013b
Liangcheng	Palaeoproterozoic granitic gneiss	1922±25 Ma.	Zhang et al., 2013a
Gushan, Datong	Neoarchaeal-Palaeoproterozoic TTG gneisses; Palaeoproterozoic charnockitic gneiss	~1852-1973 Ma; 1948±15 Ma; 1868±16 Ma; 1858±18 Ma.	Wang et al., 2015; this study
Huangtuyao, Lujiaoying, Xinghe	Neoarchaeal and Palaeoproterozoic charnockitic gneiss	1958±25 Ma; 1858±26 Ma; 1808±38 Ma; 1834±81 Ma; 1834±47 Ma.	Santosh et al., 2013; Yang et al., 2014a
Dongyanghe, Shangyi	Neoarchaeal-Palaeoproterozoic TTG gneisses	~1826-1931 Ma.	Su et al., 2014
Manjinggou, Huai'an	Neoarchaeal-Palaeoproterozoic TTG gneisses; Palaeoproterozoic granitic gneiss	1954±32 Ma; 1840-1850 Ma.	Zhao et al., 2008; Wang et al., 2010; Liu et al., 2012; Luo et al., 2012
North Hengshan	Neoarchaeal-Palaeoproterozoic TTG gneisses	1916.7±9.9 Ma; 1850-1930 Ma.	Zhang et al., 2013b
Fuping	Neoarchaeal-Palaeoproterozoic TTG gneisses; Palaeoproterozoic granitic gneiss	1820-1880 Ma.	Zhao et al., 2002; Guan et al., 2002;
Xuanhua-Tianzhen-Huai'an	Neoarchaeal-Palaeoproterozoic TTG gneisses	~1820-1850 Ma.	Liu et al., 2012
Khondalite Series			
Helanshan	Pelitic granulites, garnet-bearing feldspathic quartzite, garnet-biotite gneiss	~1950 Ma; ~1870 Ma.	Yin et al., 2011
Qilishan	High-pressure pelitic granulites, garnet-sillimanite-leucoplexites, garnet-feldspar quartzite	~1950 Ma; ~1920 Ma; ~1880 Ma.	Yin et al., 2009, 2014
Daqingshan-Wulashan	Pelitic granulites, orthopyroxene-garnet-biotite gneiss, garnet feldspathic gneiss, quartzite	~1960-1830 Ma.	Wan et al., 2009; Dong et al., 2012; Cai et al., 2015
Ji'ning	Pelite granulite	~1900-1950 Ma; ~1890; ~1870 Ma.	Li et al., 2010; Jiao et al., 2013a,b; Su et al., ; Cai et al., 2014
Tuguiwula, Tianpishan, Helinger	UHT granulites	~1920 Ma.	Santosh et al., 2007a,b, 2009b
Gushan, Datong	High-pressure pelitic granulite; Spinell-perthite-garnet granulite	~1960-1930 Ma; ~1860-1820 Ma.	Wang et al., 2015; Wu et al., 2017; this study
Huangtuyao, Xinghe	Pelitic granulite	1873 Ma; 1793 Ma (rutile age, cooling age).	Wu et al., 1998, 2006
Manjinggou, Huai'an	High-pressure pelitic granulites	~1950 Ma; ~1850 Ma; 1916±30 Ma; 1840±24 Ma.	Zhao et al., 2010
Ordos basement (drill cores)	Pelitic granulites	~1960-1930 Ma; ~1900-1880 Ma .	Wan et al., 2013; Wang et al., 2014; Gou et al., 2016; He et al., 2016
Lüliang	Pelitic granulite	~1950 Ma.	Zhao et al., 2017
Womakeng, Chicheng	High-pressure pelitic granulite	~1912 Ma.	Zhang et al., 2016b
Garnet-bearing Mafic Granulite			
Daqingshan-Wulashan	Garnet-bearing mafic granulite, mafic granulite, amphibolite	~1950 Ma, ~1900 Ma, ~1850 Ma; ~1970-1940 Ma; ~1920-1880 Ma; 1860-1840 Ma.	Liu et al., 2014, 2015
Gushan, Datong	Garnet-bearing mafic granulite	~1924-1930 Ma; 1850-1870 Ma; ~1800 Ma; 1939±15 Ma; 1835±30 Ma	Wang et al., 2015; this study
Huangtuyao, Xinghe	Garnet-bearing mafic granulite	~1900-1950 Ma; ~1850 Ma; ~1800 Ma.	Zhang et al., 2014, 2016a; Wang et al., 2016
Manjinggou, Huai'an; Xiwangshan, Xuanhua	Garnet-bearing mafic granulite	1918±20 Ma; 1827±18 Ma; ~1820-1800 Ma; ~1870 Ma.	Guo et al., 2005; this study
North Hengshan	Garnet-bearing mafic granulite	~1848-1888 Ma; ~1769-1963 Ma (weighted mean age 1873±20 Ma).	Kroner et al., 2006; Qian et al., 2017
Fuping	Garnet-bearing mafic granulite	1924±21 Ma; 1829±8 Ma; 1831±10 Ma; 1923±19 Ma; 1857±17 Ma; 1891±14 Ma; 1849±6 Ma.	Qian and Yin, 2016; Tang et al., 2017
Womakeng, Chicheng	Garnet-bearing mafic granulite	~1915 Ma.	Zhang et al., 2016b
Chengde	Garnet-bearing mafic granulite	~1870-1900 Ma; ~1810-1850 Ma.	Mao et al., 1999; Chu et al., 2012

processes (Zhang *et al.* 1994), or different tectonic slabs from independent orogens (Zhao *et al.* 2005, 2010), or different metamorphic terranes from two flanks of a high-temperature paired metamorphic belt (Liu and

Li 2009; Santosh and Kusky 2010). All of the above interpretations are based on an assumption that the varying granulites have diverse metamorphic histories. However, recent geological mapping and structural

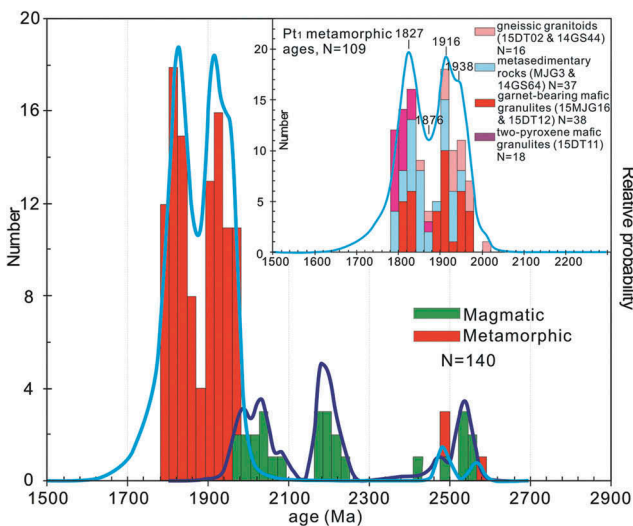


Figure 9. Histogram of zircon U–Pb ages from studied samples in this study. The histogram of late Palaeoproterozoic metamorphic ages of the varied granulite-facies samples is shown in the inset.

analyses demonstrated that these granulites had concordant deformation features (Zhang *et al.* 2014, 2016a, 2016b; Wang *et al.* 2016; Wu *et al.* 2016, 2017). Metamorphism studies also suggested these granulites suffered comparable P – T conditions and P – T loops (Figure 8; Wu 2016; Wu *et al.* 2016, 2017, 2018; Wang *et al.* 2016). In this study, zircon ages reveal that these rocks from Datong–Huai’an area have commonly documented two comparable metamorphic age populations of ~1970–1900 Ma and ~1880–1790 Ma, corresponding to approximate timing of HP granulite-facies and IP–LP granulite-facies stages, respectively. It indicates that the khondalite series, associated garnet-bearing mafic granulites, and gneissic granitoids (felsic granulites) from the study area have a common metamorphic history at least since peak metamorphic stage, although their prograde evolution is still unclear (Wu *et al.* 2016, 2018; Zhou *et al.* 2017).

Additionally, the paired occurrence of metasedimentary rocks (khondalite series), garnet-bearing mafic granulites, and gneissic granitoids has also been reported in some localities in the NCC, such as the Daqingshan–Wulashan area of Inner Mongolia (Liu *et al.* 2014, 2017), Jiaobei area in Shandong (e.g. Zhou *et al.* 2004; Tam *et al.* 2012a, 2012b; Liu *et al.* 2013; Zou *et al.* 2017), Chicheng area in Hebei (Ma and Wang 1995; Zhang *et al.* 2016b), Lüliang area (Guo 2015; Xiao *et al.* 2017; Zhao *et al.* 2017), and Wugang area in He’nan province (Lu *et al.* 2014, 2017). All existed data seemly suggest the spatially associated granulite-facies lithologies have similar metamorphic histories rather than separate ones. We therefore prefer to

interpret that these Palaeoproterozoic granulites from Datong–Huai’an area are probably formed in one single metamorphic cycle.

6.4 Reconsideration petrogenesis and tectonic implications of Palaeoproterozoic granulites from the study area

This study suggests that previous tectonic models based on contrasting metamorphic histories of these rocks need re-evaluation. In Zhao *et al.*’s (2005, 2008, 2010) model, they interpreted that the ~1950 million year metamorphic terranes (khondalite series) in Manjinggou, Huai’an area, should be tectonic nappes from the Western Block (Khondalite Belt) during the collision of the Eastern and Western Blocks at ~1850 Ma. If this model is assumed, it seems to indicate that not only the khondalite series, but also other granulite-facies rocks, such as garnet-bearing mafic granulites, TTG gneiss, and charnockitic gneiss, should stem from the Western Block. In Santosh’s (2010) interpretation, they preferred a double-side collision with scissor-like suturing model along the Ordos Block and Yinshan & Eastern Blocks, which is also supported by Zhang *et al.* (2016a). The above interpretations suggested that these Palaeoproterozoic granulites occurred as linear belts, could compare with Phanerozoic HP–UHP terranes in subduction zone, and hence they were assumed as hallmark of suture zone among blocks (e.g. Wang *et al.*, 1994; Zhai *et al.* 1994; Zhai 1998; Zhao *et al.* 1999, 2000).

However, recent studies indicate that Palaeoproterozoic granulites are widespread in the exposed basement of the NCC (Figure 10; Zhai 2009; Zhai *et al.* 2010; Guo *et al.* 2015; Wu *et al.* 2016; Zhou *et al.* 2017), and new Palaeoproterozoic granulite localities are continuously recognized (e.g. Duan *et al.* 2015; Liu *et al.* 2015, 2017; Xiao *et al.* 2017; Yang *et al.*, 2017; Zhao *et al.* 2017; Cai *et al.* 2017b). Additionally, some Palaeoproterozoic granulites are recognized in the drill cores of Phanerozoic Ordos basin (Hu *et al.* 2013; Wan *et al.*, 2013; Wang *et al.* 2014; Gou *et al.* 2016), and also some Palaeoproterozoic crustal granulite xenoliths are identified from Phanerozoic volcanics (e.g. Liu *et al.* 2001; Zheng *et al.* 2004a, 2004b; Zheng *et al.* 2008, 2012; Ying *et al.* 2010; Zhang *et al.* 2012c; Su *et al.* 2015). It seems to suggest that the distribution of Palaeoproterozoic granulites in the NCC is broad or pan-belt, rather than linear (Zhai 2009; Zhai *et al.* 2010; Guo *et al.* 2015; Wu *et al.* 2016; Zhou *et al.* 2017). It induces some recent studies to reconsider the petrogenesis and tectonic significance of the Palaeoproterozoic granulites in the north-central NCC. For example, Kusky *et al.* (2007) correlated the Palaeoproterozoic metamorphism to assembly of the NCC with rest of the Columbia supercontinent. They also stated that the scale of Palaeoproterozoic

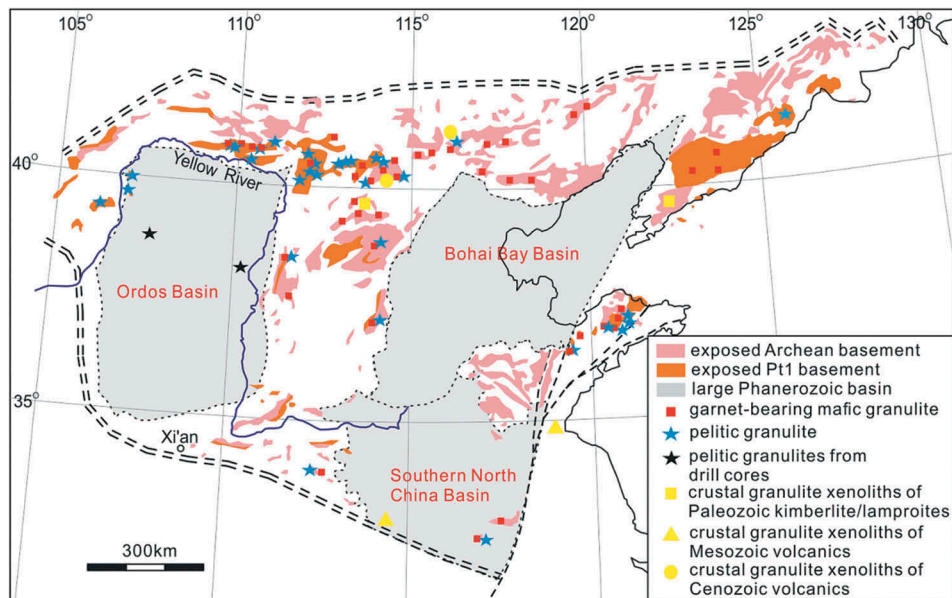


Figure 10. A summary of distribution of Palaeoproterozoic granulites (including granulites xenoliths in Phanerozoic volcanics) in the NCC, modified after Wu *et al.* (2016).

metamorphism might be pan-NCC, and the metamorphic grade is degrading from north to south in the NCC (Li *et al.* 1996; Kusky *et al.* 2007, Kusky *et al.* 2016). For instance, HT–UHT and/or IP–HP granulite-facies rocks mainly exposed in the Helanshan–Daqingshan–Liangcheng–Ji’ning and/or Hengshan–Fuping–Huai’an–Xuanhua–Chengde area to the north, and amphibolite- to greenschist-facies rocks in the Wutai–Lüliang–Zanhuang–Zhongtiao area to the south. The granulite-facies belt in the northern NCC were interpreted as exhumed root of collision-related plateau, analogous to Tibet, which were considered as southern part of the Northern Hebei Orogen (Kusky *et al.* 2007, 2016). Alternatively, Zhai and his co-authors not only emphasize the spatial distribution of these granulites in the NCC, but they also notice that these granulites exhibit relatively high apparent thermal regimes (14–28°C/km), slow exhumation, and cooling rates (0.18–0.24 mm/year), which is contrasting with counterparts of Phanerozoic HP–UHP metamorphic terranes (Zhai 2009, 2012; Zhai *et al.* 2010; Zhai and Santosh 2011; Wu 2016; Wu *et al.* 2016; Zhou *et al.* 2017). In this context, they proposed a rift–subduction–collision model (Palaeoproterozoic mobile belt) to interpret the formation and exhumation of Palaeoproterozoic granulite-facies lithologies in the NCC (Wu *et al.* 2017, 2018; Zhou *et al.* 2017). They interpret that the characteristics of Palaeoproterozoic granulite-facies metamorphism might suggest operation of incipient plate tectonics, which is likely featured by warm subduction in limited depths, possibly in crustal scales, and soft collision between smaller blocks, and the tectonic style is more or less similar with Phanerozoic plate tectonics (Zhai 2012; Wu *et al.* 2017, 2018; Zhou *et al.* 2017).

It seems that this study and previously published data are still insufficient to give an exclusive interpretation on the petrogenesis and tectonic significance of these Palaeoproterozoic granulite-facies rocks. But it makes sure that these rocks from Datong–Huai’an area have shared metamorphic histories from peak stage to subsequent retrograde stages since ~1970–1900 Ma, and exhibit crustal scale *P–T* conditions, relatively higher apparent geothermal gradients (~15–25°C/km), and slow exhumation rates (~0.1–0.3 mm/year) (Wu 2016; Wu *et al.* 2016, 2017, 2018). We therefore prefer to interpret that these granulites are probably formed in one single metamorphic cycle, which might be in response to crustal-scale subduction–collision–exhumation processes involved in Palaeoproterozoic mobile belt. Further studies are still needed before a comprehensive understanding of the tectonic implications of these granulite-facies rocks.

7. Conclusions

- (1) Zircons from a tonalitic gneiss (15DT02) document three episodes tectono-thermal events. The magmatic cores yield an upper intercept age of 2516 ± 44 Ma, representing the emplacement age of the tonalitic magma. It is followed by Archaean–Palaeoproterozoic boundary reworking, exhibiting as recrystallized domains around magmatic zircon cores, accompanying with considerable Pb loss. A few zircon rims register the late Palaeoproterozoic imprint with $^{207}\text{Pb}/^{206}\text{Pb}$ ages from 1973 to 1852 Ma. Zircons from a charnockitic gneiss

- (14GS44) show obvious core-and-rim structures. The magmatic cores yield an upper intercept age of 2197 ± 20 Ma. The metamorphic rims yield an upper intercept age of 1948 ± 15 Ma and one $^{207}\text{Pb}/^{206}\text{Pb}$ age of 1868 ± 16 Ma.
- (2) Most zircons from a kyanite-bearing pelitic granulite (MJG3) display strong recrystallization features, with low luminescence, weak core-and-rim structures, or structureless, low Th/U ratios, flat HREE patterns, indicative of their concurrent growth with garnet. The U–Pb data mainly exhibit two distinct populations. The older population yields an upper intercept age of 1916 ± 30 Ma, and the younger population yields an upper intercept age of 1840 ± 24 Ma. Few zircon cores show ambiguous oscillatory zoning, steep HREE patterns with U–Pb ages of >1980 Ma. The results are consistent well with U–Pb ages of spinel–perthite–garnet granulite, in which the U–Pb ages show three populations: (1) the oldest group is represented by detrital zircons with $^{207}\text{Pb}/^{206}\text{Pb}$ ages older than ~ 2000 Ma; (2) the younger group is characterized by the dark metamorphic zircon cores with an upper intercept age of 1929 ± 26 Ma; and (3) the youngest group is featured by the grey metamorphic zircon rims with an upper intercept age of 1822 ± 27 Ma.
- (3) Zircons from both garnet-bearing mafic granulites (15MJG16 and 15DT12) show metamorphic features with spherical to oval in shapes, sector zoning, fir-tree zoning, core-and-rim structures, or structureless. The U–Pb data show three distinct clusters. The oldest group is characterized by magmatic-like domains with $^{207}\text{Pb}/^{206}\text{Pb}$ age of >2000 Ma. The younger group is represented by metamorphic zircon cores or part of the sector zoning domains with ages of 1918 ± 20 Ma (15MJG16) and 1935 ± 15 Ma (15DT12). The youngest group is characterized by metamorphic rims with ages of 1827 ± 18 Ma (15MJG16) and 1835 ± 30 Ma (15DT12), respectively. Zircons from the two-pyroxene mafic granulite (15DT11) show elongated to oval shapes, with low luminescence, structureless, relatively narrow Th/U ratios of 0.34–0.60, and steep HREE patterns, which yield an upper intercept age of 1820 ± 37 Ma.
- (4) Our results, together with published data, suggest that the varying granulite-facies lithologies from Datong–Huai’an area have commonly imprinted the Palaeoproterozoic metamorphism at least since peak metamorphic stage, although their formation ages are different. The metamorphic ages could be divided into at least two clusters of ~ 1970 – 1900 Ma and ~ 1880 – 1790 Ma, with peaks at ~ 1916 – 1938 Ma and ~ 1827 Ma, respectively. We suggest that the timing of HP granulite-facies metamorphism is at ~ 1916 – 1938 Ma, and the timing of IP–LP granulite-facies metamorphism is culminating at ~ 1827 Ma.
- (5) The common metamorphic histories of these Palaeoproterozoic granulites from Datong–Huai’an area suggest that these granulites are probably metamorphosed during one single metamorphic cycle, which might respond to crustal-scale subduction–collision–exhumation processes involved in Palaeoproterozoic mobile belt.

Acknowledgments

This study was financially supported by research programs (Grant No. 41702196, 41530208, 41402064) by the National Natural Science Foundation of China, the National Key Research and Development Program of China (No. 2016YFC0601002) funded by the State Ministry of Science and Technology, and Special Fund for Basic Scientific Research of Central Colleges, Chang’an University, China (310827172201).

Disclosure statement

No potential conflict of interest was reported by the authors.

Funding

This work was supported by the National Natural Science Foundation of China [41402064,41530208,41702196];Special Fund for Basic Scientific Research of Central Colleges, Chang’an University, China [310827172201];National Key Research and Development Program of China [2016YFC0601002].

References

- Andersen, T., 2002, Correction of common lead in U–Pb analyses that do not report ^{204}Pb : *Chemical Geology*, v. 192, p. 59–79. doi: [10.1016/S0009-2541\(02\)00195-X](https://doi.org/10.1016/S0009-2541(02)00195-X).
- Cai, J., Liu, F., Liu, P., Wang, F., Meng, E., Wang, W., Yang, H., Ji, L., and Liu, L., 2017b, Discovery of granulite-facies metamorphic rocks in the Ji’an area, northeastern Jiao–Liao–Ji Belt, North China Craton: Metamorphic P–T evolution and geological implications: *Precambrian Research*, v. 303, p. 626–640. doi: [10.1016/j.precamres.2017.08.018](https://doi.org/10.1016/j.precamres.2017.08.018).
- Cai, J., Liu, F.L., Liu, P.H., Wang, F., and Shi, J.R., 2014, Metamorphic P–T conditions and U–Pb dating of the sillimanite–cordierite–garnet paragneisses in Sanchakou, Jining

- area, Inner Mongolia: *Acta Petrologica Sinica*, v. 30, no. 2, p. 472–490. (in Chinese with English abstract).
- Cai, J., Liu, F.L., Liu, P.H., Wang, F., and Shi, J.R., 2015, Geochronology of the Paleoproterozoic khondalite rocks from the Wulashan-Daqingshan area, the Khondalite Belt: *Acta Petrologica Sinica*, v. 31, no. 10, p. 3081–3106. (in Chinese with English abstract).
- Cai, J., Liu, P.H., Ji, L., and Shi, J.R., 2017a, Zircon geochronology of the Paleoproterozoic high-grade supracrustal rocks from the Huai'an terrane, northwestern Hebei: *Acta Petrologica Sinica*, v. 33, no. 9, p. 2811–2826. (in Chinese with English abstract).
- Chu, H., Wang, H.C., Wei, C.J., Liu, H., and Zhang, K., 2012, The metamorphic evolution of high-pressure granulites in Chengde area, northern margin of North China: Zircon chronology and geochemical evidence: *Acta Geoscientia Sinica*, v. 33, no. 6, p. 977–987. (in Chinese with English abstract).
- Corfu, F., Hanchar, J.M., Hoskin, P.W.O., and Kinny, P., 2003, Atlas of zircon textures, in Hanchar, J.M., and Hoskin, P.W.O., eds., *Zircon. Mineralogical society of America reviews in mineralogy & geochemistry*, Vol. 53, Mineralogical Society of America, p. 469–495.
- Dong, C.Y., Liu, D.Y., Li, J.J., Wan, Y.S., Zhou, H.Y., Li, C.D., Yang, Y.H., and Xie, L.W., 2007, Paleoproterozoic khondalite belt in the western North China Craton: New evidence from SHRIMP dating and Hf isotope composition of zircons from metamorphic rocks in the Byan Ul-Helan Mountains area: *Chinese Science Bulletin*, v. 52, no. 21, p. 2984–2994. doi: [10.1007/s11434-007-0404-9](https://doi.org/10.1007/s11434-007-0404-9).
- Dong, C.Y., Wan, Y.S., Xu, Z.Y., Liu, D.Y., Yang, Z.S., Ma, M.Z., and Xie, H.Q., 2012, SHRIMP zircon U-Pb dating of late Paleoproterozoic kondalites in the Daqing Mountain area on North China Craton. *Science China: Earth Sciences*, 12, 1851–1862.
- Duan, Z., Wei, C., and Qian, J., 2015, Metamorphic P-T paths and zircon U-Pb age data for the paleoproterozoic metabasic dykes of high-pressure granulite facies from eastern Hebei, North China Craton: *Precambrian Research*, v. 271, p. 295–310. doi: [10.1016/j.precamres.2015.10.015](https://doi.org/10.1016/j.precamres.2015.10.015).
- Gou, L.L., Zhang, C.L., Brown, M., Piccoli, P.M., Lin, H.B., and Wei, X.S., 2016, P-T-t evolution of pelitic gneiss from the basement underlying the northwestern Ordos basin, North China Craton, and the tectonic implications: *Precambrian Research*, v. 276, p. 67–84. doi: [10.1016/j.precamres.2016.01.030](https://doi.org/10.1016/j.precamres.2016.01.030).
- Guan, H., Sun, M., Wilde, S.A., Zhou, X.H., and Zhai, M.G., 2002, Shrimp u-pb zircon geochronology of the fuping complex: implications for formation and assembly of the north china craton. *Precambrian Research*, v. 113, p.1–18. doi: [10.1016/S0301-9268\(01\)00197-8](https://doi.org/10.1016/S0301-9268(01)00197-8).
- Guo, J.H., O'Brien, P.J., and Zhai, M.G., 2002, High-pressure granulites in the Sanggan area, North China Craton: Metamorphic evolution, P-T paths and geotectonic significance: *Journal of Metamorphic Geology*, v. 20, p. 741–756. doi: [10.1046/j.1525-1314.2002.00401.x](https://doi.org/10.1046/j.1525-1314.2002.00401.x).
- Guo, J.H., Peng, P., Chen, Y., Jiao, S.J., and Windley, B.F., 2012, UHT sapphirine granulite metamorphism at 1.93-1.92 Ga caused by gabbro intrusions: Implications for tectonic evolution of the northern margin of the North China Craton: *Precambrian Research*, v. 222-223, p. 124–142. doi: [10.1016/j.precamres.2011.07.020](https://doi.org/10.1016/j.precamres.2011.07.020).
- Guo, J.H., Sun, M., Chen, F.K., and Zhai, M.G., 2005, Sm-Nd and SHRIMP U-Pb zircon geochronology of high-pressure granulites in the Sanggan area, North China Craton: Timing of paleoproterozoic continental collision: *Journal of Asian Earth Sciences*, v. 24, p. 629–642. doi: [10.1016/j.jseaes.2004.01.017](https://doi.org/10.1016/j.jseaes.2004.01.017).
- Guo, J.H., and Zhai, M.G., 2001, Sm-Nd age dating of high-pressure granulites and amphibolites from Sanggan area, North China Craton: *Chinese Science Bulletin*, v. 46, p. 106–111. doi: [10.1007/BF03187002](https://doi.org/10.1007/BF03187002).
- Guo, J.H., Zhai, M.G., Li, J.H., and Li, Y.G., 1996, Nature of the early Precambrian Sangan Structure Zone in North China Craton: Evidence from rock association: *Acta Petrologica Sinica*, v. 12, no. 2, p. 193–207. (in Chinese with English abstract).
- Guo, J.H., Zhai, M.G., Li, Y.G., and Yan, Y.H., 1998, Contrasting metamorphic P-T paths of Archean high-pressure granulites from the North China Craton: Metamorphism and tectonic significance: *Acta Petrologica Sinica*, v. 14, no. 4, p. 430–448. (in Chinese with English abstract).
- Guo, J.H., Zhai, M.G., Peng, P., Jiao, S.J., Zhao, L., and Wang, H. Z., 2015, Paleoproterozoic granulites in the North China Craton and their geological implications, in: Zhai, M., (ed.), *Precambrian geology of China*, Springer Berlin Heidelberg, p. 137–169.
- Guo, J.H., Zhai, M.G., Zhang, Y.G., Li, Y.G., Yan, Y.H., and Zhang, W.H., 1993, Early Precambrian Manjinggou high-pressure granulite melange belt on the south edge of the Huaian complex, North China craton: Geological features, petrology and isotopic geochronology: *Acta Petrologica Sinica*, v. 9, p. 329–341. (in Chinese with English abstract).
- Guo, X.J., 2015, Paleoproterozoic granulite facies metamorphism for gneisses from Lüliang complex in Xiyupi area and its tectonic significance [Master thesis]: Xi'an, China, Northwest University, 1–65p. (in Chinese with English abstract)
- He, X.F., Santosh, M., Bockmann, K., Kelsey, D.E., Hand, M., Hu, J.M., and Wan, Y.S., 2016, Petrology, phase equilibria and monazite geochronology of granulite-facies metapelites from deep drill cores in the ordos block of the north china craton. *Lithos*, v. 262, p. 44-57. doi: [10.1016/j.lithos.2016.06.022](https://doi.org/10.1016/j.lithos.2016.06.022).
- Hoskin, P.W.O., and Black, L.P., 2000, Metamorphic zircon formation by solid-state recrystallization of protolith igneous zircon: *Journal of Metamorphic Geology*, v. 18, p. 423–439. doi: [10.1046/j.1525-1314.2000.00266.x](https://doi.org/10.1046/j.1525-1314.2000.00266.x).
- Hu, J.M., Liu, X.S., Li, Z.H., Zhao, Y., Zhang, S.H., Liu, X.C., Qu, H. J., and Chen, H., 2013, SHRIMP U-Pb zircon dating of the Ordos Basin basement and its tectonic significance: *Chinese Science Bulletin*, v. 58, p. 118–127. doi: [10.1007/s11434-012-5274-0](https://doi.org/10.1007/s11434-012-5274-0).
- Jiao, S.J., Guo, J.H., Harley, S.L., and Peng, P., 2013b, Geochronology and trace element geochemistry of zircon, monazite and garnet from the garnetite and/or associated other high-grade rocks: Implications for Palaeoproterozoic tectonothermal evolution of the khondalite series belt, North China Craton: *Precambrian Research*, v. 237, no. 7, p. 78–100. doi: [10.1016/j.precamres.2013.09.008](https://doi.org/10.1016/j.precamres.2013.09.008).

- Jiao, S.J., Guo, J.H., Harley, S.L., and Windley, B.F., 2013a, New constraints from garnetite on the P-T path of the Khondalite Belt: Implications for the tectonic evolution of the North China Craton: *Journal of Petrology*, v. 54, no. 9, p. 1725–1758. doi: [10.1093/petrology/egt029](https://doi.org/10.1093/petrology/egt029).
- Jin, W., 2002, The late paleoproterozoic orogeny in the North China Craton: *Gondwana Research*, v. 5, no. 1, p. 95–99. doi: [10.1016/S1342-937X\(05\)70893-5](https://doi.org/10.1016/S1342-937X(05)70893-5).
- Kröner, A., Cui, W.Y., Wang, S.Q., Wang, C.Q., and Nemchin, A. A., 1998, Single zircon ages from high-grade rocks of the Jianping Complex, Liaoning Province, NE China: *Journal of Asian Earth Science*, v. 16, p. 519–532. doi: [10.1016/S0743-9547\(98\)00033-6](https://doi.org/10.1016/S0743-9547(98)00033-6).
- Kröner, A., Wilde, S.A., Zhao, G.C., O'Brien, P.J., Sun, M., Liu, D. Y., Wan, Y.S., Liu, S.W., and Guo, J.H., 2006, Zircon geochronology of mafic dykes in the Hengshan Complex of northern China: Evidence for late Palaeoproterozoic rifting and subsequent high-pressure event in the North China Craton: *Precambrian Research*, v. 146, p. 45–67. doi: [10.1016/j.precamres.2006.01.008](https://doi.org/10.1016/j.precamres.2006.01.008).
- Kusky, T.M., Li, J.H., and Santosh, M., 2007, The Paleoproterozoic North Hebei Orogen: North China Craton's collisional suture with the Columbia supercontinent: *Gondwana Research*, v. 12, p. 4–28. doi: [10.1016/j.gr.2006.11.012](https://doi.org/10.1016/j.gr.2006.11.012).
- Kusky, T.M., Polat, A., Windley, B.F., Burke, K.C., Dewey, J.F., Kidd, W.S.F., Maruyama, S., Wang, J.P., Deng, H., Wang, Z.S., Wang, C., Fu, D., Li, X.W., and Peng, H.T., 2016, Insights into the tectonic evolution of the north china craton through comparative tectonic analysis: A record of outward growth of Precambrian continents: *Earth-Science Reviews*, v. 162, p. 387–432. doi: [10.1016/j.earscirev.2016.09.002](https://doi.org/10.1016/j.earscirev.2016.09.002).
- Li, J.H., Zhai, M.G., Qian, X.L., and Guo, J.H., 1998, The geological occurrence, regional tectonic setting and exhumation of late Archean high pressure granulite with the high grade metamorphic terranes, north to central portion of North China craton: *Acta Petrologica Sinica*, v. 14, p. 176–189. (in Chinese with English abstract).
- Li, X.P., Yang, Z.Y., Zhao, G.C., Grapes, R., and Guo, J.H., 2010, Geochronology of khondalite-series rocks of the Jining complex: Confirmation of depositional age and tectono-metamorphic evolution of the North China craton: *International Geology Review*, v. 53, p. 1194–1211. doi: [10.1080/00206810903548984](https://doi.org/10.1080/00206810903548984).
- Li, X.W., and Wei, C.J., 2018, Ultrahigh-temperature metamorphism in the Tuguiwula area, Khondalite Belt, North China Craton. *Journal of Metamorphic Geology*, v. 00, p. 1–21. doi: [10.1111/jmg.12301](https://doi.org/10.1111/jmg.12301).
- Liu, F., Guo, J.H., Peng, P., and Qian, Q., 2012, Zircon U-Pb ages and geochemistry of the Huai'an TTG gneisses terrane: Petrogenesis and implications for 2.5 Ga crustal growth in the North China Craton: *Precambrian Research*, v. 213, p. 225–244. doi: [10.1016/j.precamres.2012.06.006](https://doi.org/10.1016/j.precamres.2012.06.006).
- Liu, F.L., Liu, P.H., Wang, F., Liu, C.H., and Cai, J., 2015, Progresses and overviews of voluminous metasedimentary series within the Paleoproterozoic Jiao-Liao-Ji orogenic/mobile belt, North China Craton: *Acta Petrologica Sinica*, v. 31, p. 2816–2846. (in Chinese with English abstract).
- Liu, F.L., Shen, Q.H., and Zhao, Z.R., 2002, Evolution of mineral assemblages of khondalite series in the process of prograde metamorphism, southern Inner Mongolia: *Geological Bulletin of China*, v. 21, p. 75–78. (in Chinese with English abstract).
- Liu, J.H., Liu, F.L., Ding, Z.J., Chen, J.Q., Liu, P.H., Shi, J.R., Cai, J., and Wang, F., 2013b, Zircon U-Pb chronology, geochemistry and their petrogenesis of early Paleoproterozoic granitoid gneisses in Ulashan area, North China Craton: *Acta Petrologica Sinica*, v. 29, no. 2, p. 485–500. (in Chinese with English abstract).
- Liu, P.H., Liu, F.L., Cai, J., Liu, C.H., Liu, J.H., Wang, F., Xiao, L.L., and Shi, J.R., 2017, Spatial distribution, P–T paths, and tectonic significance of high-pressure mafic granulites from the Daqingshan–Wulashan Complex in the Khondalite Belt, North China Craton: *Precambrian Research*, v. 303, p. 687–708. doi: [10.1016/j.precamres.2017.09.004](https://doi.org/10.1016/j.precamres.2017.09.004).
- Liu, P.H., Liu, F.L., Liu, C.H., Liu, J.H., Wang, F., Xiao, L.L., and Cai, J., 2014, Multiple mafic magmatic and high-grade metamorphic events revealed by zircons from meta-mafic rocks in the Daqingshan–Wulashan Complex of the Khondalite Belt, North China Craton: *Precambrian Research*, v. 246, no. 6, p. 334–357. doi: [10.1016/j.precamres.2014.02.015](https://doi.org/10.1016/j.precamres.2014.02.015).
- Liu, P.H., Liu, F.L., Wang, F., Liu, J.H., Yang, H., Cai, J., and Shi, J.R., 2013, Petrogenesis, P–T path, and tectonic significance of high-pressure mafic granulites from the Jiaobei terrane, North China Craton: *Precambrian Research*, v. 233, p. 237–258. doi: [10.1016/j.precamres.2013.05.003](https://doi.org/10.1016/j.precamres.2013.05.003).
- Liu, S., Santosh, M., Wang, W., Bai, X., and Yang, P., 2011, Zircon U–Pb chronology of the Jianping Complex: Implications for the Precambrian crustal evolution history of the northern margin of North China Craton: *Gondwana Research*, v. 20, no. 1, p. 48–63. doi: [10.1016/j.gr.2011.01.003](https://doi.org/10.1016/j.gr.2011.01.003).
- Liu, S.J., Dong, C.Y., Xu, Z.Y., Santosh, M., Ma, M.Z., Xie, H.Q., Liu, D.Y., and Wan, Y.S., 2013a, Palaeoproterozoic episodic magmatism and high-grade metamorphism in the North China Craton: Evidence from SHRIMP zircon dating of magmatic suites in the Daqingshan area: *Geological Journal*, v. 48, no. 5, p. 429–455. doi: [10.1002/gj.v48.5](https://doi.org/10.1002/gj.v48.5).
- Liu, S.J., and Li, J.H., 2009, Paleoproterozoic high temperature paired metamorphic belt in central part of Southern Inner Mongolia and its tectonic implication: *Geological Journal of China Universities*, v. 15, p. 48–56. (in Chinese with English abstract).
- Liu, S.J., Li, J.H., and Santosh, M., 2008, Ultrahigh temperature metamorphism of Tuguiwula khondalite belt, Inner Mongolia: Metamorphic reaction texture and P–T indication: *Acta Petrologica Sinica*, v. 24, no. 6, p. 1185–1192. (in Chinese with English abstract).
- Liu, X.S., Jin, W., and Li, S.X., 1992, Low-pressure metamorphism of granulite facies in an early Proterozoic orogenic event in central Inner Mongolia: *Acta Geologica Sinica*, v. 66, no. 3, p. 244–256. (in Chinese with English abstract).
- Liu, Y.S., Gao, S., Jin, S.Y., Hu, S.H., Sun, M., Zhao, Z.B., and Feng, J.L., 2001, Geochemistry and petrogenesis of lower crustal xenoliths from Hannuoba, North China: Implications for the continental lower crustal composition and evolution at convergent margin: *Geochimica Et Cosmochimica Acta*, v. 65, no. 15, p. 2589–2604. doi: [10.1016/S0016-7037\(01\)00609-3](https://doi.org/10.1016/S0016-7037(01)00609-3).

- Lu, J.S., Wang, G.D., Wang, H., Chen, H.X., and Wu, C.M., 2014, Palaeoproterozoic metamorphic evolution and geochronology of the Wugang block, southeastern terminal of the Trans-North China Orogen: *Precambrian Research*, v. 251, p. 197–211. doi: [10.1016/j.precamres.2014.06.015](https://doi.org/10.1016/j.precamres.2014.06.015).
- Lu, J.S., Zhai, M.G., Lu, L.S., Wang, H.Y., Chen, H.X., Peng, T., Wu, C.M., and Zhao, T.P., 2017, Metamorphic P-T-t path retrieved from metapelites in the southeastern Taihua metamorphic complex, and the Paleoproterozoic tectonic evolution of the southern North China Craton: *Journal of Asian Earth Sciences*, v. 134, p. 352–364. doi: [10.1016/j.jseaes.2016.12.001](https://doi.org/10.1016/j.jseaes.2016.12.001).
- Lu, L.Z., Jin, S.Q., Xu, X.C., and Liu, F.L., 1991, The genesis of early Precambrian khondalite series in southeastern Inner Mongolia and its potential mineral resources: Changchun, Jilin scientific and technical Publishing House, 1–157p. (in Chinese).
- Lu, L.Z., Xu, X.C., and Liu, F.L., 1996, The Precambrian Khondalite series in Northern China: Changchun, Changchun Publishing House, 16–125p. (in Chinese).
- Ludwig, K.R., 2012. User's Manual for Isoplot 3.75: A geochronological toolkit for Microsoft Excel: Berkeley Geochronology Center Special Publication No. 5, 74.
- Luo, Z.B., Zhang, H.F., Diwu, C.R., and Zhang, H., 2012, Zircon U-Pb, Lu-Hf isotope and trace element compositions of intermediate pyroxene granulite in the Huai'an area, Northwest Hebei Province: Constraints on the timing of retrograde metamorphism: *Acta Petrologica Sinica*, v. 28, no. 11, p. 3721–3738. (in Chinese with English abstract).
- Ma, J., and Wang, R.M., 1995, The discovery of coexisting kyanite + perthite assemblage in Xuanhua-Chicheng high-pressure granulite belt and its geological significance: *Acta Petrologica Sinica*, v. 11, no. 3, p. 273–278. (in Chinese with English abstract).
- Ma, M.Z., Wan, Y.S., Santosh, M., Xu, Z.Y., Xie, H.Q., Dong, C.Y., Liu, D.Y., and Guo, C.L., 2012, Decoding multiple tectonothermal events in zircons from single rock samples: Shrimp zircon U-Pb data from the late neoproterozoic rocks of Daqingshan, North China Craton: *Gondwana Research*, v. 22, no. 3–4, p. 810–827. doi: [10.1016/j.gr.2012.02.020](https://doi.org/10.1016/j.gr.2012.02.020).
- Mao, D.B., Zhong, C.T., Chen, Z.H., Lin, Y.X., Li, H.M., and Hu, X. D., 1999. Isotopic ages and geological implications of high-pressure mafic granulites in the northern Chengde area, Hebei Province, China. *Acta Petrologica Sinica* 15, 524–534.
- O'Brien, P.J., Walte, N., and Li, J., 2005, The petrology of two distinct granulite types in the hengshan mts, china, and tectonic implications: *Journal of Asian Earth Sciences*, v. 24, no. 5, p. 615–627. doi: [10.1016/j.jseaes.2004.01.002](https://doi.org/10.1016/j.jseaes.2004.01.002).
- Peng, P., Guo, J.H., Zhai, M.G., and Bleeker, W., 2010, Palaeoproterozoic gabbro-noritic and granitic magmatism in the northern margin of the North China Craton: Evidence of crust-mantle interaction: *Precambrian Research*, v. 183, p. 635–659. doi: [10.1016/j.precamres.2010.08.015](https://doi.org/10.1016/j.precamres.2010.08.015).
- Qian, J.H., Wei, C.J., and Yin, C.Q., 2017, Paleoproterozoic P-T-t evolution in the Hengshan-Wutai-Fuping area, North China Craton: Evidence from petrological and geochronological data: *Precambrian Research*, v. 303, p. 91–104. doi: [10.1016/j.precamres.2017.02.016](https://doi.org/10.1016/j.precamres.2017.02.016).
- Qian, J.H., and Yin, C.Q., 2016. High-pressure granulites in the fuping complex of North China Craton: Metamorphic P-T-t evolution and tectonic implications, in Abstract Volume of 2015 Annual meeting of Chinese Geoscience Union: Beijing, p. 213.
- Qu, M., Guo, J.H., Lai, Y., Peng, P., and Liu, F., 2012, Origin and geological significance of the 1.81 Ga hyalophane-rich pegmatite veins from the high-pressure granulite terrain in the Central Zone of North China Craton: *Science China Earth Science*, v. 55, p. 193–203. doi: [10.1007/s11430-011-4330-y](https://doi.org/10.1007/s11430-011-4330-y).
- Rubatto, D., 2002, Zircon trace element geochemistry: Partitioning with garnet and the link between U-Pb ages and metamorphism: *Chemical Geology*, v. 184, p. 123–138. doi: [10.1016/S0009-2541\(01\)00355-2](https://doi.org/10.1016/S0009-2541(01)00355-2).
- Santosh, M., 2010, Assembling North China Craton within the Columbia supercontinent: The role of double-sided subduction: *Precambrian Research*, v. 178, p. 149–167. doi: [10.1016/j.precamres.2010.02.003](https://doi.org/10.1016/j.precamres.2010.02.003).
- Santosh, M., and Kusky, T., 2010, Origin of paired high pressure-ultrahigh-temperature orogens: A ridge subduction and slab window model: *Terra Nova*, v. 22, p. 35–42. doi: [10.1111/j.1365-3121.2009.00914.x](https://doi.org/10.1111/j.1365-3121.2009.00914.x).
- Santosh, M., Liu, D.Y., Shi, Y.R., and Liu, S.J., 2013, Paleoproterozoic accretionary orogenesis in the North China Craton: A SHRIMP zircon study: *Precambrian Research*, v. 227, p. 29–54. doi: [10.1016/j.precamres.2011.11.004](https://doi.org/10.1016/j.precamres.2011.11.004).
- Santosh, M., Liu, S.J., Tsunogae, T., and Li, J.H., 2012, Paleoproterozoic ultrahigh-temperature granulites in the North China Craton: Implications for tectonic models on extreme crustal metamorphism: *Precambrian Research*, v. 222–223, no. 223, p. 77–106. doi: [10.1016/j.precamres.2011.05.003](https://doi.org/10.1016/j.precamres.2011.05.003).
- Santosh, M., Sajeev, K., Li, J.H., Liu, S.J., and Itaya, T., 2009a, Counterclockwise exhumation of a hot orogen: The Paleoproterozoic ultrahigh-temperature granulites in the North China Craton: *Lithos*, v. 110, no. 1–4, p. 140–152. doi: [10.1016/j.lithos.2008.12.010](https://doi.org/10.1016/j.lithos.2008.12.010).
- Santosh, M., Tsunogae, T., Li, J.H., and Liu, S.J., 2007a, Discovery of sapphirine-bearing Mg-Al granulites in the North China Craton: Implications for Paleoproterozoic ultrahigh temperature metamorphism: *Gondwana Research*, v. 11, p. 263–285. doi: [10.1016/j.gr.2006.10.009](https://doi.org/10.1016/j.gr.2006.10.009).
- Santosh, M., Wan, Y., Liu, D., Dong, C., and Li, J., 2009b, Anatomy of zircons from an ultrahot orogen: The amalgamation of the North China Craton within the supercontinent Columbia: *Journal of Geology*, v. 117, p. 429–443. doi: [10.1086/598949](https://doi.org/10.1086/598949).
- Santosh, M., Wilde, S.A., and Li, J.H., 2007b, Timing of Paleoproterozoic ultrahigh-temperature metamorphism in the North China Craton: Evidence from SHRIMP U-Pb zircon geochronology: *Precambrian Research*, v. 159, p. 178–196. doi: [10.1016/j.precamres.2007.06.006](https://doi.org/10.1016/j.precamres.2007.06.006).
- Shimizu, H., Tsunogae, T., Santosh, M., Liu, S.J., and Li, J.H., 2013, Phase equilibrium modelling of Palaeoproterozoic ultrahigh-temperature sapphirine granulite from the Inner Mongolia Suture Zone, North China Craton: Implications for counterclockwise P-T path: *Geological Journal*, v. 48, p. 456–466. doi: [10.1002/gj.v48.5](https://doi.org/10.1002/gj.v48.5).
- Su, Y., Zheng, J., Wei, Y., Li, Y., Ping, X., and Huang, Y., 2015, Deep-seated crustal xenoliths record multiple Paleoproterozoic tectonothermal events in the northern

- North China Craton: Precambrian Research, v. 270, p. 318–333. doi: [10.1016/j.precamres.2015.09.021](https://doi.org/10.1016/j.precamres.2015.09.021).
- Su, Y.P., Zheng, J.P., Griffin, W.L., Zhao, J.H., Li, Y.L., Wei, Y., and Huang, Y., 2014, Zircon U-Pb ages and Hf isotope of gneissic rocks from the Huai'an Complex: Implications for crustal accretion and tectonic evolution in the northern margin of the North China Craton: Precambrian Research, v. 255, p. 335–354. doi: [10.1016/j.precamres.2014.10.007](https://doi.org/10.1016/j.precamres.2014.10.007).
- Sun, S.S., and McDonough, W.F., 1989, Chemical and isotopic systematics of oceanic basalts: Implications for mantle composition and processes, in Saunders, A.D., and Norry, M.J., Eds., Magmatism in the Ocean Basins: Vol. 42, Geol. Soc. Spec. Publ., London, p. 313–345.
- Tam, P.Y., Zhao, G.C., Sun, M., Li, S.Z., Wu, M.L., and Yin, C.Q., 2012b, Petrology and metamorphic P-T path of high-pressure mafic granulites from the Jiaobei massif in the Jiao-Liao-Ji Belt, North China Craton: Lithos, v. 155, p. 94–109. doi: [10.1016/j.lithos.2012.08.018](https://doi.org/10.1016/j.lithos.2012.08.018).
- Tam, P.Y., Zhao, G.C., Zhou, X.W., Sun, M., Guo, J.H., Li, S.Z., Yin, C.Q., Wu, M.L., and He, Y.H., 2012a, Metamorphic P-T path and implications of high-pressure pelitic granulites from the Jiaobei massif in the Jiao-Liao-Ji Belt, North China Craton: Gondwana Research, v. 22, p. 104–117. doi: [10.1016/j.gr.2011.09.006](https://doi.org/10.1016/j.gr.2011.09.006).
- Tang, L., Santosh, M., Tsunogae, T., Koizumi, T., Hu, X.K., and Teng, X.M., 2017, Petrology, phase equilibria modelling and zircon U-Pb geochronology of Paleoproterozoic mafic granulites from the Fuping Complex, North China Craton: Journal Metamorph Geological, v. 35, p. 517–540. doi: [10.1111/jmg.12243](https://doi.org/10.1111/jmg.12243).
- Trap, P., Faure, M., Lin, W., Augier, R., and Fouassier, A., 2011, Syn-collisional channel flow and exhumation of paleoproterozoic high pressure rocks in the Trans-North China Orogen: The critical role of partial-melting and orogenic bending: Gondwana Research, v. 20, no. 2–3, p. 498–515. doi: [10.1016/j.gr.2011.02.013](https://doi.org/10.1016/j.gr.2011.02.013).
- Tsunogae, T., Liu, S.J., Santosh, M., Shimizu, H., and Li, J.H., 2011, Ultrahigh-temperature metamorphism in Daqingshan, Inner Mongolia Suture Zone, North China Craton: Gondwana Research, v. 20, p. 36–47. doi: [10.1016/j.gr.2011.03.001](https://doi.org/10.1016/j.gr.2011.03.001).
- Vavra, G., Schmid, R., and Gebauer, D., 1999, Internal morphology, habit and U-Th-Pb microanalysis of amphibolite-to-granulite facies zircons: Geochronology of the Ivrea Zone (Southern Alps): Contrib Mineral Petrol, v. 134, p. 380–404. doi: [10.1007/s004100050492](https://doi.org/10.1007/s004100050492).
- Wan, Y., Liu, D., Dong, C., Xu, Z., Wang, Z., Wilde, S.A., Yang, Y., Liu, Z., and Zhou, H., 2009, The Precambrian Khondalite Belt in the Daqingshan area, North China Craton: Evidence for multiple metamorphic events in the Palaeoproterozoic era, in Reddy, S.M., Mazumder, R., and Evans, D.A.D., eds., Paleoproterozoic supercontinents and global evolution, Geological society: London, Special Publications, Vol. 323, p. 73–97.
- Wan, Y.S., Song, B., Liu, D.Y., Wilde, S.A., Wu, J.S., Shi, Y.R., Yin, X.Y., and Zhou, H.Y., 2006, SHRIMP U-Pb zircon geochronology of Palaeoproterozoic metasedimentary rocks in the North China Craton: Evidence for a major Late Palaeoproterozoic tectonothermal event: Precambrian Research, v. 149, p. 249–271. doi: [10.1016/j.precamres.2006.06.006](https://doi.org/10.1016/j.precamres.2006.06.006).
- Wan, Y.S., Xie, H.Q., Yang, H., Wang, Z.J., Liu, D.Y., Kröner, A., Wide, S.A., Geng, Y.S., Sui, L. Y., Ma, M.Z., Liu, S.J., Dong, C.Y., and Du, L.L., 2013, Is the ordos block archaic or paleoproterozoic in age? implications for the precambrian evolution of the north china craton. American Journal Of Science, v. 313, p. 83–711. doi:[10.2475/07.2013.03](https://doi.org/10.2475/07.2013.03).
- Wang, H.Z., Zhang, H.F., Zhai, M.G., Oliveira, E.P., Ni, Z.Y., Zhao, L., Wu, J.L., and Cui, X.H., 2016, Granulite facies metamorphism and crust melting in the Huai'an terrane at ~1.95 Ga, North China Craton: New constraints from geology, zircon U-Pb, Lu-Hf isotope and metamorphic conditions of granulites: Precambrian Research, v. 286, p. 126–151. doi: [10.1016/j.precamres.2016.09.012](https://doi.org/10.1016/j.precamres.2016.09.012).
- Wang, J., Wu, Y.B., Gao, S., Peng, M., Liu, X.C., Zhao, L.S., Zhou, L., Hu, Z.C., Gong, H.J., and Liu, Y.S., 2010, Zircon U-Pb and trace element data from rocks of the Huai'an Complex: New insights into the late Paleoproterozoic collision between the Eastern and Western Blocks of the North China Craton: Precambrian Research, v. 178, p. 59–71. doi: [10.1016/j.precamres.2010.01.007](https://doi.org/10.1016/j.precamres.2010.01.007).
- Wang, L.J., Guo, J.H., Peng, P., and Liu, F., 2011, Metamorphic and geochronological study of garnet-bearing basic granulites from Gushan, the eastern end of the Khondalite series Belt in the North China Craton: Acta Petrologica Sinica, v. 27, p. 3689–3700. (in Chinese with English abstract).
- Wang, L.J., Guo, J.H., Peng, P., Liu, F., and Windley, B.F., 2015, Lithological units at the boundary zone between the Jining and Huai'an complexes (central-northern margin of the North China Craton): A Paleoproterozoic tectonic mélange?: Lithos, v. 227, p. 205–224. doi: [10.1016/j.lithos.2015.04.006](https://doi.org/10.1016/j.lithos.2015.04.006).
- Wang, R.M., Chen, Z.Z., and Chen, F., 1991, Grey tonalitic gneiss and high-pressure granulite inclusions in hengshan, Shanxi Province and their geological significance: Acta Petrologica Sinica, v. 11, p. 36–44. (in Chinese with English abstract).
- Wang, W., Liu, X.H., Hu, J.M., Li, Z.H., Zhao, Y., Zhai, M.G., Liu, X. C., Clarke, G., Zhang, S.H., and Qu, H.J., 2014, Late Paleoproterozoic medium-P high grade metamorphism of basement rocks beneath the northern margin of the Ordos Basin, NW China: Petrology, phase equilibrium modelling and U-Pb geochronology: Precambrian Research, v. 251, p. 181–196. doi: [10.1016/j.precamres.2014.06.016](https://doi.org/10.1016/j.precamres.2014.06.016).
- Wei, C.J., Qian, J.H., and Zhou, X.W., 2014, Paleoproterozoic crustal evolution of the Hengshan-Wutai-Fuping region, North China Craton. Geoscience Frontiers 54, 85–97.
- Wei, Y., Zheng, J.P., Su, Y.P., and Ma, Q., 2013, Zircon U-Pb ages and Hf isotopes of granulites from the Huai'an Complex: Implications for the accretion and reworking of the lower crust beneath the northern margin of the North China Craton: Acta Petrologica Sinica, v. 29, p. 2281–2294. (in Chinese with English abstract).
- Wu, C.H., 2007, Meta-sedimentary rocks and tectonic division of the North China Craton: Geological Journal of China Universities, v. 13, no. 3, p. 442–457. (in Chinese with English abstract).
- Wu, C.H., Gao, Y.D., Mei, H.L., and Zhong, C.T., 1994, Structural features and unconformity arguments between the khondalite suite and the granulite complex in Huangtuyao area, Nei Mongol, North China, in Qian, X.L. and Wang, R.M., eds., Geological evolution of granulite belt in northern of North

- China Craton: Beijing, Seismological Press, p. 145–156. (in Chinese with English abstract).
- Wu, C.H., and Zhong, C.T., 1998, Early Proterozoic SW-NE collision model for the central part of the North China Craton: Implications for tectonic regime of the Khondalite downward into lower crust in Jin-Meng high-grade region: *Progress in Precambrian Research*, v. 21, no. 3, p. 28–49. (in Chinese with English abstract).
- Wu, J., Zhai, M., Zhang, H., Guo, J., Wang, H., Yang, W., Zhang, H., and Hu, B., 2018, Petrologic indicators of prograde metamorphism in Paleoproterozoic garnet mafic granulites from the Huai'an complex, North China Craton: *Science Bulletin*, v. 63, p. 81–84. doi: [10.1016/j.scib.2017.12.017](https://doi.org/10.1016/j.scib.2017.12.017).
- Wu, J., Zhang, H., Zhai, M., Guo, J., Li, R., Wang, H., Zhao, L., Jia, X., Wang, L., Hu, B., and Zhang, H., 2017, Paleoproterozoic high-pressure-high-temperature pelitic granulites from Datong in the North China Craton and their geological implications: Constraints from petrology and phase equilibrium modeling: *Precambrian Research*, v. 303, p. 727–748. doi: [10.1016/j.precamres.2017.09.011](https://doi.org/10.1016/j.precamres.2017.09.011).
- Wu, J.L., 2016, Metamorphism and geological implications of Paleoproterozoic HT-HP granulites from Huai'an-Datong area, the North China Craton [Ph.D. thesis]: Xi'an, ChinaNorthwest University, 1–134p. (in Chinese with English abstract).
- Wu, J.L., Zhang, H.F., Zhai, M.G., Guo, J.H., Liu, L., Yang, W.Q., Wang, H.Z., Zhao, L., Jia, X.L., and Wang, W., 2016, Discovery of pelitic high-pressure granulite from Manjinggou of the Huai'an Complex, North China Craton: Metamorphic P-T evolution and geological implications: *Precambrian Research*, v. 278, p. 323–336. doi: [10.1016/j.precamres.2016.03.001](https://doi.org/10.1016/j.precamres.2016.03.001).
- Xia, X.P., Sun, M., Zhao, G.C., and Luo, Y., 2006, LA-ICP-MS U-Pb geochronology of detrital zircons from the Jining Complex, North China craton and its tectonic significance: *Precambrian Research*, v. 144, p. 199–212. doi: [10.1016/j.precamres.2005.11.004](https://doi.org/10.1016/j.precamres.2005.11.004).
- Xia, X.P., Sun, M., Zhao, G.C., Wu, F.Y., Xu, P., Zhang, J., and He, Y.H., 2008, Paleoproterozoic crustal growth in the western block of the North China craton: Evidence from detrital zircon Hf and whole-rock Sr-Nd isotopic compositions of the khondalites from the Jining complex: *American Journal of Science*, v. 308, p. 304–327. doi: [10.2475/03.2008.05](https://doi.org/10.2475/03.2008.05).
- Xiao, L.L., Clarke, G., Liu, F.L., and Wu, C.M., 2017, Discovery of mafic granulite in the Guandishan area of the Lüliang complex, North China Craton: Age and metamorphic evolution: *Precambrian Research*, v. 303, p. 604–625. doi: [10.1016/j.precamres.2017.08.020](https://doi.org/10.1016/j.precamres.2017.08.020).
- Xiao, L.L., and Liu, F.L., 2015, Precambrian metamorphic history of the metamorphic complexes in the Trans-North China Orogen, North China Craton: *Acta Petrologica Sinica*, v. 31, no. 10, p. 3012–3044. (in Chinese with English abstract).
- Xu, Z.Y., Wan, Y.S., Dong, C.Y., Ma, M.Z., and Liu, D.Y., 2015, Late Neoproterozoic magmatism identified in Daqingshan, Inner Mongolia: Shrimp zircon U-Pb dating: *Acta Petrologica Sinica*, v. 31, no. 6, p. 1509–1517. (in Chinese with English abstract).
- Yan, Y.H., Zhai, M.G., and Guo, J.H., 1991, The cordierite-sillimanite assemblages in the Archean granulite belt on North China Platform as an indicator for low-pressure granulite facies: *Acta Petrologica Sinica*, v. 4, p. 47–56. (in Chinese with English abstract).
- Yang, C., and Wei, C., 2017, Two phases of granulite facies metamorphism during the Neoproterozoic and Paleoproterozoic in the East Hebei, North China Craton: Records from mafic granulites: *Precambrian Research*, v. 301, p. 49–64. doi: [10.1016/j.precamres.2017.09.005](https://doi.org/10.1016/j.precamres.2017.09.005).
- Yang, Q.Y., Santosh, M., and Tsunogae, T., 2014a, First report of Paleoproterozoic incipient charnockite from the North China Craton: Implications for ultrahigh-temperature metasomatism: *Precambrian Research*, v. 243, p. 168–180. doi: [10.1016/j.precamres.2014.01.004](https://doi.org/10.1016/j.precamres.2014.01.004).
- Yang, Q.Y., Santosh, M., and Tsunogae, T., 2014b, Ultrahigh-temperature metamorphism under isobaric heating: New evidence from the North China Craton: *Journal of Asian Earth Sciences*, v. 95, p. 2–16. doi: [10.1016/j.jseaes.2014.01.018](https://doi.org/10.1016/j.jseaes.2014.01.018).
- Yin, C.Q., Zhao, G.C., Guo, J.H., Sun, M., Zhou, X.W., Zhang, J., Xia, X.P., and Liu, C.H., 2011, U-Pb and Hf isotopic study of zircons of the Helanshan complex: Constrains on the evolution of the khondalite belt in the Western block of the North China Craton: *Lithos*, v. 122, p. 25–38. doi: [10.1016/j.lithos.2010.11.010](https://doi.org/10.1016/j.lithos.2010.11.010).
- Yin, C.Q., Zhao, G.C., and Sun, M., 2015, High-pressure pelitic granulites from the Helanshan complex in the Khondalite Belt, North China Craton: Metamorphic P-T path and tectonic implications: *American Journal of Science*, v. 315, no. 9, p. 846–879. doi: [10.2475/09.2015.03](https://doi.org/10.2475/09.2015.03).
- Yin, C.Q., Zhao, G.C., Sun, M., Xia, X.P., Wei, C.J., Zhou, X.W., and Leung, W.H., 2009, LA-ICPMS U-Pb zircon ages of the Qianlishan Complex: Constrains on the evolution of the Khondalite Belt in the Western block of the North China Craton: *Precambrian Research*, v. 174, p. 78–94. doi: [10.1016/j.precamres.2009.06.008](https://doi.org/10.1016/j.precamres.2009.06.008).
- Yin, C.Q., Zhao, G.C., Wei, C.J., Sun, M., Guo, J.H., and Zhou, X.W., 2014, Metamorphism and partial melting of high pressure pelitic granulites from the Qianlishan complex: Constraints on the tectonic evolution of the Khondalite Belt in the North China Craton: *Precambrian Research*, v. 242, p. 172–186. doi: [10.1016/j.precamres.2013.12.025](https://doi.org/10.1016/j.precamres.2013.12.025).
- Ying, J.F., Zhang, H.F., and Tang, Y.J., 2010, Lower crustal xenoliths from Junan, Shandong province and their bearing on the nature of the lower crust beneath the North China Craton: *Lithos*, v. 119, no. 3–4, p. 363–376. doi: [10.1016/j.lithos.2010.07.015](https://doi.org/10.1016/j.lithos.2010.07.015).
- Zhai, M., Hu, B., Zhao, T., Peng, P., and Meng, Q., 2015, Late paleoproterozoic–Neoproterozoic multi-rifting events in the north china craton and their geological significance: A study advance and review: *Tectonophysics*, v. 662, p. 153–166. doi: [10.1016/j.tecto.2015.01.019](https://doi.org/10.1016/j.tecto.2015.01.019).
- Zhai, M., and Santosh, M., 2013, Metallogeny of the north china craton: Link with secular changes in the evolving earth: *Gondwana Research*, v. 24, no. 1, p. 275–297. doi: [10.1016/j.gr.2013.02.007](https://doi.org/10.1016/j.gr.2013.02.007).
- Zhai, M.G., 1991, The main characteristics of granulites in north China and the orientation of further research on them: *Acta Petrologica Sinica*, v. 4, p. 66–77. (in Chinese with English abstract).
- Zhai, M.G., 1997, Recent advances in the study of granulites from the North China craton: *International Geological Review*, v. 39, p. 325–341. doi: [10.1080/00206819709465275](https://doi.org/10.1080/00206819709465275).
- Zhai, M.G., 1998, There important high-pressure and high-temperature metamorphic zones in China and their

- geotectonic significance: *Acta Petrologica Sinica*, v. 14, no. 4, p. 419–429. (In Chinese with English abstract).
- Zhai, M.G., 2009, Two kinds of granulites (HT-HP and HT-UHT) in North China Craton: Their genetic relation and geotectonic implications: *Acta Petrologica Sinica*, v. 25, p. 1753–1771. (In Chinese with English abstract).
- Zhai, M.G., 2012, Evolution of the North China Craton and early plate tectonics: *Acta Geologica Sinica*, v. 86, no. 9, p. 1335–1349. (In Chinese with English abstract).
- Zhai, M.G., Guo, J.H., Li, J.H., Li, Y.G., Yan, Y.H., and Zhang, W. H., 1995, Archean retrograded eclogite and its implications from the North China Craton: *Chinese Science Bulletin*, v. 40, p. 1590–1594. (In Chinese).
- Zhai, M.G., Guo, J.H., and Li, Y.G., 1994, High-pressure granulite zone and related rock association in Jin-Ji-Inner Mongolia joint area, in Qian, X.L., and Wang, R.M., eds., *Geological evolution of granulite facies zone in northern North China*: Beijing, Seismological Press, p. 21–31. (In Chinese with English abstract).
- Zhai, M.G., Guo, J.H., Yan, Y.H., Li, Y.G., and Han, X.L., 1992, The discovery of high-pressure basic granulite in the Archaean north China Craton and preliminary study: *Sciences in China*, v. 12, p. 1325–1330. (In Chinese).
- Zhai, M.G., Li, T.S., Peng, P., Hu, B., Liu, F., Zhang, Y.B., and Guo, J. H., 2010, Precambrian key tectonic events and evolution of the North China Craton, in Kusky, T.M., Zhai, M.G., and Xiao, W.J., Eds., *The evolving continents*: Vol. 338, Geological Society of London Special Publications, p. 235–262.
- Zhai, M.G., and Santosh, M., 2011, Early Precambrian odyssey of the North China Craton: A synoptic overview: *Gondwana Research*, v. 20, p. 6–25. doi: [10.1016/j.gr.2011.02.005](https://doi.org/10.1016/j.gr.2011.02.005).
- Zhang, D.D., Guo, J.H., Tian, Z.H., and Liu, F., 2016b, Metamorphism and P-T evolution of high pressure granulite in Chicheng, northern part of the Paleoproterozoic Trans-North China Orogen: *Precambrian Research*, v. 280, p. 76–94. doi: [10.1016/j.precamres.2016.04.009](https://doi.org/10.1016/j.precamres.2016.04.009).
- Zhang, H.F., Luo, Z.B., and Wang, H.Z., 2013b, Paleoproterozoic 2.0 Ga metagranite in the Liangcheng area, Inner Mongolia: Constraints on regional ultra-high temperature metamorphism: *Acta Petrologica Sinica*, v. 29, no. 7, p. 2391–2404. (In Chinese with English abstract).
- Zhang, H.F., Luo, Z.B., Zhou, Z.G., and Liu, C.F., 2009, Palaeoproterozoic collisional time in the Sanggan area of the North China Craton: Constraints from age of regional ductile shearing and post-collisional strongly peraluminous granites: *Journal of Mineralogy and Petrology*, v. 1, p. 60–67. (In Chinese with English abstract).
- Zhang, H.F., Wang, H.Z., Santosh, M., and Zhai, M.G., 2016a, Zircon U-Pb ages of Paleoproterozoic mafic granulites from the Huai'an terrane, North China Craton (NCC): Implications for timing of cratonization: *Precambrian Research*, v. 272, p. 244–263. doi: [10.1016/j.precamres.2015.11.004](https://doi.org/10.1016/j.precamres.2015.11.004).
- Zhang, H.F., Ying, J.F., Santosh, M., and Zhao, G.C., 2012c, Episodic growth of precambrian lower crust beneath the North China Craton: A synthesis: *Precambrian Research*, v. 222–223, p. 255–264. doi: [10.1016/j.precamres.2011.04.006](https://doi.org/10.1016/j.precamres.2011.04.006).
- Zhang, H.F., Zhai, M.G., and Peng, P., 2006, Zircon SHRIMP U-Pb age of the Paleoproterozoic high-pressure granulites from the Sanggan area, North China craton and its geologic implications: *Earth Science Frontiers*, v. 13, p. 190–199. (In Chinese with English abstract).
- Zhang, H.F., Zhai, M.G., Santosh, M., DiWu, C.R., and Li, S.R., 2012a, Low-Al and high-Al trondhjemites in the Huai'an Complex, North China Craton: Geochemistry, zircon U-Pb and Hf isotopes, and implications for Neoproterozoic crustal growth and remelting: *Journal of Asian Earth Sciences*, v. 49, p. 203–213. doi: [10.1016/j.jseas.2011.11.004](https://doi.org/10.1016/j.jseas.2011.11.004).
- Zhang, H.F., Zhai, M.G., Santosh, M., Di-Wu, C.R., and Li, S.R., 2011, Geochronology and petrogenesis of Neoproterozoic potassic meta-granites from Huai'an Complex: Implications for the evolution of the North China Craton: *Gondwana Research*, v. 20, p. 82–105. doi: [10.1016/j.gr.2011.01.009](https://doi.org/10.1016/j.gr.2011.01.009).
- Zhang, H.F., Zhai, M.G., Santosh, M., Wang, H.Z., Zhao, L., and Ni, Z.Y., 2014, Paleoproterozoic granulites from the Xinghe graphite mine, North China Craton: Geology, zircon U-Pb geochronology and implications for the timing of deformation, mineralization and metamorphism: *Ore Geology Reviews*, v. 63, p. 478–497. doi: [10.1016/j.oregeorev.2014.03.014](https://doi.org/10.1016/j.oregeorev.2014.03.014).
- Zhang, H.T., Li, J.H., Liu, S.J., Li, W.S., Santosh, M., and Wang, H. H., 2012b, Spinel + quartz-bearing ultrahigh-temperature granulites from Xumayao, Inner Mongolia Suture Zone, North China Craton: Petrology, phase equilibria and counterclockwise P-T path: *Geoscience Frontiers*, v. 3, no. 5, p. 603–611. doi: [10.1016/j.gsf.2012.01.003](https://doi.org/10.1016/j.gsf.2012.01.003).
- Zhang, J.S., Dirks, P.H.G.M., and Passchier, C.W., 1994, Extensional collapse and uplift of a polymetamorphic granulite terrain in the Archean of north China: *Precambrian Research*, v. 67, p. 37–57. doi: [10.1016/0301-9268\(94\)90004-3](https://doi.org/10.1016/0301-9268(94)90004-3).
- Zhang, Y.H., Wei, C.J., Tian, W., and Zhou, X.W., 2013a, Reinterpretation of metamorphic age of the Hengshan Complex, North China Craton: *Chinese Science Bulletin*, v. 58, p. 4300–4307. doi: [10.1007/s11434-013-5993-x](https://doi.org/10.1007/s11434-013-5993-x).
- Zhao, G.C., Cawood, P.A., Li, S.Z., Wilde, S.A., Sun, M., Zhang, J., He, Y.H., and Yin, C.Q., 2012, Amalgamation of the North China Craton: Key issues and discussion: *Precambrian Research*, v. 222–223, p. 55–76. doi: [10.1016/j.precamres.2012.09.016](https://doi.org/10.1016/j.precamres.2012.09.016).
- Zhao, G.C., Cawood, P.A., Wilde, S.A., and Lu, L.Z., 2000, Metamorphism of basement rocks in the Central Zone of the North China Craton: Implications for Paleoproterozoic tectonic evolution: *Precambrian Research*, v. 103, p. 55–88. doi: [10.1016/S0301-9268\(00\)00076-0](https://doi.org/10.1016/S0301-9268(00)00076-0).
- Zhao, G.C., Cawood, P.A., Wilde, S.A., and Lu, L.Z., 2001, High-pressure granulites (retrograded eclogites) from the Hengshan Complex, North China Craton: Petrology and tectonic implications: *Journal of Petrology*, v. 42, p. 1141–1170. doi: [10.1093/petrology/42.6.1141](https://doi.org/10.1093/petrology/42.6.1141).
- Zhao, G.C., Sun, M., Wilde, S.A., and Li, S.Z., 2005, Late Archean to Paleoproterozoic evolution of the North China Craton: Key issues revisited: *Precambrian Research*, v. 136, p. 177–202. doi: [10.1016/j.precamres.2004.10.002](https://doi.org/10.1016/j.precamres.2004.10.002).
- Zhao, G.C., Sun, M., Wilde, S.A., Li, S.Z., Liu, S.W., and Zhang, J., 2006, Composite nature of the North China Granulite-Facies Belt: Tectonothermal and geochronological constraints: *Gondwana Research*, v. 9, p. 337–348. doi: [10.1016/j.gr.2005.10.004](https://doi.org/10.1016/j.gr.2005.10.004).
- Zhao, G.C., Wilde, S.A., Cawood, P.A., et al., 1999, Thermal evolution of two types of mafic granulites from the North China craton: Implications for both mantle plume and collisional tectonics: *Geological Magazine*, vol. 136, p. 223–240. doi: [10.1017/S001675689900254X](https://doi.org/10.1017/S001675689900254X).

- Zhao, G.C., Wilde, S.A., and Cawood Sun, M., 2002. Shrimp U-Pb zircon ages of the fuping complex: implications for accretion and assembly of the north china craton. *American Journal Of Science* 302, 191-226. doi: [10.1016/S0301-9268\(01\)00197-8](https://doi.org/10.1016/S0301-9268(01)00197-8).
- Zhao, G.C., Wilde, S.A., Guo, J.H., Cawood, P.A., Sun, M., and Li, X.P., 2010. Single zircon grains record two continental collisional events in the North China Craton: *Precambrian Research*, v. 177, p. 266–276. doi: [10.1016/j.precamres.2009.12.007](https://doi.org/10.1016/j.precamres.2009.12.007).
- Zhao, G.C., Wilde, S.A., Sun, M., Guo, J.H., Kröner, A., Li, S.Z., Li, X.P., and Wu, C.M., 2008. SHRIMP U-Pb zircon geochronology of the Huai'an Complex: Constraints on Late Archean to Paleoproterozoic crustal accretion and collision of the Trans-North China Orogen: *American Journal of Science*, v. 308, p. 270–303. doi: [10.2475/03.2008.04](https://doi.org/10.2475/03.2008.04).
- Zhao, J., Gou, L.L., Zhang, C.L., Guo, A.L., Guo, X.J., and Liu, X.Y., 2017. P-T-t path and tectonic significance of pelitic migmatites from the Lüliang complex in Xiyupi area of Trans-North China Orogen, North China Craton: *Precambrian Research*, v. 303, p. 573–589. doi: [10.1016/j.precamres.2017.07.010](https://doi.org/10.1016/j.precamres.2017.07.010).
- Zhao, Z.P., ed, 1993. *The Precambrian crustal evolution*, Science Publishing House, Beijing, 1–330p. (in Chinese with English abstract).
- Zheng, J.P., Griffin, W.L., Ma, Q., O'Reilly, S.Y., Xiong, Q., Tang, H.Y., Zhao, J.H., Yu, C.M., and Su, Y.P., 2012. Accretion and reworking beneath the North China Craton: *Lithos*, v. 149, p. 61–78. doi: [10.1016/j.lithos.2012.04.025](https://doi.org/10.1016/j.lithos.2012.04.025).
- Zheng, J.P., Griffin, W.L., O'Reilly, S.Y., Hu, B.Q., Zhang, M., Tang, H.Y., Su, Y.P., Zhang, Z.H., Pearson, N., Wang, F.Z., and Lu, F.X., 2008. Continental collision and accretion recorded in the deep lithosphere of central China: *Earth and Planetary Science Letters*, v. 269, p. 496–506. doi: [10.1016/j.epsl.2008.03.003](https://doi.org/10.1016/j.epsl.2008.03.003).
- Zheng, J.P., Griffin, W.L., O'Reilly, S.Y., Lu, F.X., Yu, C.M., Zhang, M., and Li, H.M., 2004b. U-Pb and Hf-isotope analysis of zircons in mafic xenoliths from Fuxian kimberlites: Evolution of the lower crust beneath the North China craton: *Contributions Mineral Petrol*, v. 148, p. 79–103. doi: [10.1007/s00410-004-0587-x](https://doi.org/10.1007/s00410-004-0587-x).
- Zheng, J.P., Lu, F.X., and Yu, C.M., 2004a. An in situ zircon Hf isotope, U-Pb age and trace element study of banded granulite xenoliths from Hannuoba basalt: tracking the early evolution of the lower crust in the North China craton. *Chinese Sciences Bulletin* 49, 277–285.
- Zhong, C.T., 1999. The geological features and origin of two-stage-high-pressure basic granulite from the Shanxi-Hebei-Inner Mongolia terrain in North China Craton: *Progress in Precambrian Research*, v. 22, no. 2, p. 53–58. (in Chinese with English abstract).
- Zhou, L.G., Zhai, M.G., Lu, J.S., Zhao, L., Wang, H.Z., Wu, J.L., Liu, B., Shan, H.X., and Cui, X.H., 2017. Paleoproterozoic metamorphism of high-grade granulite facies rocks in the North China Craton: Study advances, questions and new issues: *Precambrian Research*, v. 303, p. 520–547. doi: [10.1016/j.precamres.2017.06.025](https://doi.org/10.1016/j.precamres.2017.06.025).
- Zhou, X.W., Wei, C.J., Geng, Y.S., and Zhang, L.F., 2004. Discovery and implications of the high pressure pelitic granulite from the Jiaobei massif: *Chinese Science Bulletin*, v. 49, p. 1942–1948. doi: [10.1007/BF03184286](https://doi.org/10.1007/BF03184286).
- Zou, Y., Zhai, M., Santosh, M., Zhou, L., Zhao, L., Lu, J., and Shan, H., 2017. High-pressure pelitic granulites from the Jiao-Liao-Ji Belt, North China Craton: A complete PT path and its tectonic implications: *Journal of Asian Earth Sciences*, v. 134, p. 103–121. doi: [10.1016/j.jseas.2016.10.015](https://doi.org/10.1016/j.jseas.2016.10.015).